



CERN-EP-2025-066
20 March 2025

Measurement of correlations among net-charge, net-proton, and net-kaon multiplicity distributions in Pb–Pb collisions at $\sqrt{s_{NN}} = 5.02$ TeV

ALICE Collaboration*

Abstract

Correlations among conserved quantum numbers, such as the net-electric charge, the net-baryon, and the net-strangeness in heavy-ion collisions, are crucial for exploring the QCD phase diagram. In this letter, these correlations are investigated using net-proton number (as a proxy for the net-baryon), net-kaon number (for the net-strangeness), and net-charged particle number in Pb–Pb collisions at $\sqrt{s_{NN}} = 5.02$ TeV with the ALICE detector. The observed correlations deviate from the Poissonian baseline, with a more pronounced deviation at LHC energies than at RHIC. Theoretical calculations of the Thermal-FIST hadron resonance gas model, HIJING, and EPOS LHC event generators are compared with experimental results, where a significant impact of resonance decays is observed. Thermal-FIST calculations under the grand canonical and canonical ensembles highlight significant differences, underscoring the role of local charge conservation in explaining the data. Recent lattice QCD studies have demonstrated that the magnetic field generated by spectator protons in heavy-ion collisions affects susceptibility ratios, in particular those related to the net-electric charge and the net-baryon numbers. The experimental findings are in qualitative agreement with the expectations of lattice QCD.

arXiv:2503.18743v1 [nucl-ex] 24 Mar 2025

© 2025 CERN for the benefit of the ALICE Collaboration.

Reproduction of this article or parts of it is allowed as specified in the CC-BY-4.0 license.

*See Appendix A for the list of collaboration members

1 Introduction

Fluctuations and correlations among quantum numbers: the net-electric charge (Q), the net-baryon (B), and the net-strangeness (S), reveal key properties of strongly interacting matter [1–8]. These quantities play a crucial role in understanding the phase structure of quantum chromodynamics (QCD), as they can be studied both in experimental heavy-ion collisions and by first-principle lattice QCD (LQCD) calculations via thermodynamic susceptibilities [9–13]. At LHC energies, where the baryon chemical potential (μ_B) is close to zero [14], the transition from the low-temperature hadronic phase to the high-temperature quark–gluon plasma (QGP) phase is predicted to be an analytic crossover by LQCD [15]. At larger values of μ_B , a first-order phase transition line is anticipated [16]. The first-order phase transition line is expected to end at a critical point (CP) [17–19], near which the thermodynamic susceptibilities show a divergent behavior [20–22]. Determining the precise location of the CP remains an active area of research, pursued through both experimental measurements and theoretical studies. Fluctuations and correlations of net-conserved charges serve as sensitive probes for analyzing freeze-out conditions in heavy-ion collisions and may help elucidate their connection to the QCD phase transition [23, 24]. Active experimental programs, such as the RHIC Beam Energy Scan (BES) and the LHC, are extensively investigating these using cumulant analyses [25–29].

The cumulants ($\kappa_{\alpha,\beta}^{lm}$) of net-multiplicity distributions for associated conserved charges (α, β) can be arranged in a matrix form, where diagonal cumulants quantify fluctuations of individual conserved charges, and off-diagonal cumulants capture correlations between different conserved charges. They are related to the corresponding thermodynamic susceptibilities ($\chi_{\alpha,\beta}^{lm}$) by the equation:

$$\chi_{\alpha,\beta}^{lm} = \frac{1}{VT^3} \kappa_{\alpha,\beta}^{lm}, \quad (1)$$

where V and T denote the volume and temperature of the thermodynamic system. This study focuses on second-order fluctuations and correlations, with κ_{α}^2 and $\kappa_{\alpha,\beta}^{11}$ measured using the relations:

$$\kappa_{\alpha}^2 = \langle (\delta N_{\alpha})^2 \rangle, \quad (2)$$

and

$$\kappa_{\alpha,\beta}^{11} = \langle (\delta N_{\alpha})(\delta N_{\beta}) \rangle, \quad (3)$$

where $\delta N_{\alpha} = (N_{\alpha^+} - N_{\alpha^-}) - \langle (N_{\alpha^+} - N_{\alpha^-}) \rangle$ and angular brackets $\langle \dots \rangle$ denote average over all events. The use of cumulant ratios eliminates the temperature and volume dependence and enables a more direct comparison between experimental results and theoretical models. Since not all baryons and strange particles can be measured experimentally, the net-proton (calculated as $\Delta p = N_p - N_{\bar{p}}$) and net-kaon (calculated as $\Delta K = N_{K^+} - N_{K^-}$) numbers are used as proxies for the net-baryon and the net-strangeness numbers, respectively. The net-charged particle (ΔQ) is defined as the sum of net-pion (calculated as $\Delta \pi = N_{\pi^+} - N_{\pi^-}$), net-kaon, and net-proton, i.e., $\Delta Q = \Delta \pi + \Delta K + \Delta p$. The impact of other hadrons on the diagonal and off-diagonal susceptibilities associated with Q, B, and S studied with the Hadron Resonance Gas (HRG) model can be found in Ref. [30]. The importance of investigating off-diagonal cumulants was highlighted in Ref. [5] through studies of baryon-strangeness correlations; $C_{B,S} = -3\chi_{B,S}^{11}/\chi_S^2$, referred to as ‘‘Koch ratio’’. The STAR experiment at RHIC has reported correlations among net-charged particle, net-proton, and net-kaon, i.e., $C_{p,K} = \kappa_{p,K}^{11}/\kappa_K^2$, $C_{Q,K} = \kappa_{Q,K}^{11}/\kappa_K^2$, and $C_{Q,p} = \kappa_{Q,p}^{11}/\kappa_p^2$ in Au+Au collisions at $\sqrt{s_{NN}} = 7.7$ to 200 GeV [31]. Since the off-diagonal cumulants $\kappa_{Q,K}^{11}$ and $\kappa_{Q,p}^{11}$ inherently include the diagonal cumulants of net-kaons and net-protons respectively, the ratios $C_{Q,K}$ and $C_{Q,p}$ can be expanded as:

$$C_{Q,K} = \frac{\kappa_{p,K}^{11}}{\kappa_K^2} + \frac{\kappa_{\pi,K}^{11}}{\kappa_K^2} + 1, \quad (4)$$

and

$$C_{Q,p} = \frac{\kappa_{p,K}^{11}}{\kappa_p^2} + \frac{\kappa_{\pi,p}^{11}}{\kappa_p^2} + 1. \quad (5)$$

At LHC energies, the off-diagonal cumulants are directly related to the balance function (BF) integrals [32, 33]. Moreover, they are sensitive to various dynamical effects, which may obscure the critical fluctuations of interest. These effects include correlations arising from global and local conservation of quantum numbers [34, 35], volume fluctuations [36], resonance decays [37, 38], fluctuations in the initial state [39], thermal blurring [40], among other possible contributions. Thus, isolating and understanding the specific contributions of these fluctuations and correlations is crucial to make accurate inferences about the QCD phase structure and its critical behaviors.

In experiments, electric charge, baryon number, and strangeness are conserved in each event over the full acceptance. Consequently, fluctuations in the net-conserved charges vanish in the full phase space due to global conservation laws and must instead be studied within a restricted phase space, which can be achieved by selecting specific ranges in rapidity (y) and/or transverse momentum (p_T) of the detected particles [41]. While global charge conservation effects are suppressed in small acceptance windows, the acceptance should not be smaller than the system's intrinsic dynamical correlation length, as this may mask the fluctuations of interest [36]. The acceptance fraction (α_{acc}), defined as the ratio of the phase space covered by kinematic cuts to the system's total phase space [36, 42, 43], plays an important role in understanding how the measured fluctuations and correlations relate to the theoretical calculations of grand-canonical susceptibilities within HRG models and LQCD calculations. Moreover, event-by-event fluctuations in net-particle numbers can be influenced by fluctuations in the number of target and projectile participants for a given centrality selection [44]. The effect of participant fluctuations (also known as volume fluctuations) on cumulants of the net-conserved charges has been studied within the framework of the Wounded Nucleon Model [45] in Ref. [36]. It was found that the cumulants are significantly affected by volume fluctuations at lower energies. In contrast, at LHC energies, where the mean net-particle numbers vanish, the cumulants are independent of volume fluctuations up to third order.

In the early stages of high-energy heavy-ion collisions with non-zero impact parameters, a strong magnetic field is generated by the spectator nucleons. At LHC energies, the field strength is estimated to reach $eB \sim 15m_\pi^2 \sim 10^{15}$ T [46]. This field is transient and decays rapidly with time [47, 48]. However, a QGP medium with finite electrical conductivity can partially sustain it [49, 50], making the decay rate dependent on the medium's conductivity, which remains experimentally unconstrained. Depending on the electrical conductivity and the formation time of the QGP medium created in heavy-ion collisions, the initial magnetic field may influence the motion of final-state particles. There is considerable interest in understanding how such intense magnetic fields influence the properties and dynamics of final-state hadrons. Recently, LQCD calculations have indicated that such a magnetic field can influence specific combinations of susceptibilities related to electric charge, baryon number, and strangeness, which can be studied experimentally in peripheral heavy-ion collisions [51]. In the absence of a magnetic field, up (u) and down (d) quarks exhibit isospin symmetry, i.e., they interact with the strong nuclear force in the same way. However, the introduction of a magnetic field breaks this symmetry because of the different electric charges of the quarks, leading to changes in the quark-level susceptibilities (χ_u^2 and χ_d^2), which alter the entire second-order susceptibility matrix for electric charge, baryon number, and strangeness [51]. To study the effect of the magnetic field in the later (hadronic) stages of heavy-ion collisions, examining the centrality dependence of quantities such as $(2\chi_{Q,S}^{11} - \chi_{B,S}^{11})/\chi_S^2$, $(2\chi_{Q,B}^{11} - \chi_{B,S}^{11})/\chi_B^2$, and $\chi_{Q,B}^{11}/\chi_Q^2$ has recently been proposed in Refs. [51, 52]. In particular, the scaled ratio $[\chi_{Q,B}^{11}/\chi_Q^2(eB)]/[\chi_{Q,B}^{11}/\chi_Q^2(eB=0)]$, which shows significant deviations from unity, may serve as a sensitive indicator of the magnetic field's effect [52]. Experimentally, these quantities are accessed via proxies $(2\kappa_{Q,K}^{11} - \kappa_{p,K}^{11})/\kappa_K^2$, $(2\kappa_{Q,p}^{11} - \kappa_{p,K}^{11})/\kappa_p^2$, and $(\kappa_{Q,p}^{11}/\kappa_Q^2)/(\kappa_{Q,p}^{11}/\kappa_Q^2)^{0-5\%}$. The latter quantity $(\kappa_{Q,p}^{11}/\kappa_Q^2)/(\kappa_{Q,p}^{11}/\kappa_Q^2)^{0-5\%}$ represents the ratio of $\kappa_{Q,p}^{11}/\kappa_Q^2$ to its value in the 0–5% centrality interval.

The article is organized as follows. Section 2 provides a concise overview of the ALICE detector setup, focusing on the sub-detectors that are essential for this analysis. Details about the dataset and analysis —

including event and track selection criteria, particle identification, the efficiency correction procedure, and the estimation of statistical and systematic uncertainties, are also elaborated. The discussion on measurements and their comparison with HIJING and EPOS LHC event generators, as well as an HRG model Thermal-FIST can be found in Sec. 3. Finally, Sec. 4 summarizes the major findings of this analysis.

2 Experimental setup and data analysis

A comprehensive overview of the ALICE apparatus is available in Refs. [53, 54]. The relevant detectors used in this analysis are the Inner Tracking System (ITS) [55], a silicon detector comprising 6 cylindrical layers positioned near the collision point, the Time Projection Chamber (TPC) [56], a gaseous detector serving as ALICE's primary tracking and particle identification (PID) detector, and the Time-Of-Flight (TOF) [57] detector, a gaseous type parallel plate chamber used for PID in the intermediate momentum range. Lastly, the V0 detector [58, 59], consisting of two arrays (named V0A and V0C) of 32 scintillator tiles, is employed for triggering, event selection, and centrality determination. These arrays are located on either side of the interaction point, covering the pseudorapidity intervals $-3.7 < \eta < -1.6$ and $2.8 < \eta < 5.1$, respectively. Collision events are chosen using a minimum-bias (MB) trigger, requiring hits in both the V0A and V0C scintillators. Additionally, events with the primary vertex positioned within 10 cm relative to the nominal interaction point along the beam axis are exclusively selected to leverage the full detector acceptance. To ensure optimal detector performance, events with more than one reconstructed primary interaction vertex, referred to as pileup events [60], are excluded. A total of approximately 80 million MB events are selected for the analysis. These events are categorized into centrality intervals based on the amplitude distribution measured in the V0 detector, corresponding to hadronic interactions as described in Ref. [61]. The measurements are performed in 18 centrality intervals from 0% to 90%, each with a width of 5%.

Nestled within a solenoid that generates a magnetic field of up to 0.5 T along the beam axis, ITS, TPC, and TOF provide complete azimuthal coverage for the charged particles in the pseudorapidity interval $|\eta| < 0.8$. Particles with at least one space point in the two innermost layers of the ITS and a minimum of 70 out of 159 space points in the TPC are selected for the analysis. To further refine the track selection and minimize contamination from secondary particles (i.e., particles originating from weak decays and material interactions), a p_T -dependent selection criterion is applied to the distance of the closest approach to the primary vertex in the perpendicular plane (DCA_{xy}) to the beam axis. Tracks are selected if their DCA_{xy} is less than $DCA_{xy}(p_T) = 0.0105 + 0.035/p_T^{1.1}$ in cm. The largest allowed longitudinal distance of the tracks to the primary vertex (DCA_z) is 2 cm. Additionally, the chi-square (χ^2) per space point in the TPC and the ITS resulting from the track fit must be below 2.5 and 36, respectively.

Pions (π^+), kaons (K^+), and protons (p) (as well as their antiparticles, π^- , K^- , and \bar{p}) are identified based on the specific energy loss dE/dx in the TPC's gas volume and the flight time of a particle from the primary vertex of the collision to the TOF detector. The p_T ranges for π^\pm and K^\pm are restricted to $0.2 < p_T < 2.0$ GeV/c, while for p(\bar{p}), it is $0.4 < p_T < 2.0$ GeV/c. The variable $n(\sigma_i^{\text{TPC}})$ quantifies the PID response in the TPC, representing the deviation between the measured and expected dE/dx for a given particle species i , normalized by the detector resolution $\sigma(\text{TPC})$. The expected dE/dx is calculated using a parameterized Bethe-Bloch function [54]. The π^\pm and K^\pm are identified with $|n(\sigma_i^{\text{TPC}})| < 2$ in the range $0.2 < p_T < 0.5$ GeV/c whereas the p(\bar{p}) is selected using $|n(\sigma_i^{\text{TPC}})| < 2$ for $0.4 < p_T < 0.6$ GeV/c. The lower limit for p_T is imposed because the reconstruction efficiency becomes very low and decreases rapidly below 0.2 GeV/c [62]. Additionally, a threshold of 0.4 GeV/c is applied for protons to reduce contributions from protons generated by interactions of charged particles with the detector material. Given that TPC's particle identification is limited to low momenta (where distinct dE/dx bands are observed for different particle species), the TOF detector's information is also utilized for identifying tracks with p_T exceeding 0.5 GeV/c (0.6 GeV/c for protons). Similar to the TPC, $n(\sigma_i^{\text{TOF}})$ represents the

normalized difference between the measured and expected flight time of a particle species. Consequently, in the $0.5 < p_T < 2.0$ GeV/c range ($0.6 < p_T < 2.0$ GeV/c for protons), particle species are chosen if $|n(\sigma_i^{\text{TPC+TOF}})| < 2$, where $n(\sigma_i^{\text{TPC+TOF}}) = \sqrt{n(\sigma_i^{\text{TPC}})^2 + n(\sigma_i^{\text{TOF}})^2}$. These selection criteria ensure that the integrated purity of the selected samples of π^+ , K^+ , and p (and their antiparticles) remains above 98% across the p_T ranges used in the analysis. The efficiencies for selecting the particles depend on both p_T and event centrality, ranging from 78%, 50%, and 80% at $p_T \sim 0.5$ GeV/c to 38%, 30%, and 40% at $p_T \sim 1.0$ GeV/c for π^\pm , K^\pm , and p(\bar{p}), respectively.

The results presented are based on data from Pb–Pb collisions at $\sqrt{s_{\text{NN}}} = 5.02$ TeV, collected by the ALICE collaboration during the Run 2 data-taking period of the LHC in 2015. The net-particle numbers for pion, kaon, and proton ($\Delta\pi$, ΔK , and Δp) are measured event-by-event. Using these values, the associated cumulants (including both diagonal and off-diagonal) and the correlations $C_{p,K}$, $C_{Q,K}$, and $C_{Q,p}$ are determined for different centrality intervals. The measurements are corrected for particle detection efficiency using the analytical correction method described in Refs. [63, 64], which assumes efficiency losses governed by the binomial statistics. The efficiency correction procedure was validated in two steps by a full Monte Carlo (MC) simulation using the HIJING [65] event generator, where the generated particles are transported through the ALICE detector geometry modeled with GEANT4 [66] and reconstructed similarly to the collision data. First, the efficiencies for both particles and antiparticles of each species were determined independently as a function of p_T for each centrality interval. Then, the diagonal and off-diagonal cumulants obtained from the reconstructed MC tracks were corrected on a track-by-track basis using these efficiencies and the analytical expressions detailed in Refs. [63, 67]. An agreement of over 99% was achieved between the efficiency-corrected results from the MC-reconstructed and those from the MC-generated data.

The uncertainties in the measurements include both statistical and systematic components. A bootstrap approach [68] is employed to evaluate statistical uncertainties. The systematic uncertainties are estimated by tightening and loosening the event and track selection criteria. The uncertainties related to the event selection stem from the position of the event vertex along the beam direction and the presence of pileup events. These contributions remain below 2% across all centralities. To account for the systematic uncertainty in estimating the collision centrality, the centrality intervals are redefined using the midrapidity multiplicity distribution [69]. This modification introduces an uncertainty of up to 7% in peripheral and less than 4% in central collisions. The effects of the track selection are explored by varying the selection criteria on DCA, the number of reconstructed space points in the TPC, and the quality of the track fit, from their nominal values. Increasing the required number of TPC space points has a negligible effect, while variations in the DCA of the tracks in both transverse and longitudinal directions result in a system-

Table 1: Contributions from various systematic uncertainty sources on $C_{p,K}$, $C_{Q,K}$, and $C_{Q,p}$ in Pb–Pb collisions at $\sqrt{s_{\text{NN}}} = 5.02$ TeV. The ranges correspond to the minimum and maximum values across different centrality interval.

Sources of systematic uncertainty	$C_{p,K}$ (in %)	$C_{Q,K}$ (in %)	$C_{Q,p}$ (in %)
Vertex z -position	0.9–1.4	<0.5	<0.2
Centrality estimator	1.3–6.9	0.1–0.8	0.3–1.3
Pileup rejection	0.1–1.4	<0.3	<0.2
Space points in TPC	0.6–3.8	<0.5	<0.2
χ^2 per space point in TPC	0.7–1.2	<0.4	<0.2
χ^2 per space point in ITS	0.3–2.8	<0.4	<0.2
DCA _{xy} & DCA _z	1.6–3.9	0.4–1.2	0.3–1.0
PID	1.8–5.6	0.4–1.4	0.6–1.6
Total	5.5–8.8	0.8–2.1	1.1–1.8

atic uncertainty of 1 to 3%. The alteration of the χ^2 per space point value in the TPC and the ITS leads to uncertainties of less than 2 and 4%, respectively, across all centralities. Systematic uncertainties due to PID are assessed by varying the default selection criteria on $n(\sigma_i^{\text{TPC}})$ and $n(\sigma_i^{\text{TPC+TOF}})$ for each particle species. The default selection criterion is 2σ , which is varied to 2.5σ , resulting in uncertainties ranging from 3% to 6%, depending on centrality. Finally, considering each source's contribution as uncorrelated, the total systematic uncertainty on the observables is determined by adding them in quadrature. Table 1 shows the summary of the contributions to the total systematic uncertainty on $C_{p,K}$, $C_{Q,K}$, and $C_{Q,p}$.

3 Results

This analysis investigates the centrality dependence of the correlations $C_{p,K}$, $C_{Q,K}$, and $C_{Q,p}$, for two different p_T ranges, referred to as Set 1 and Set 2. In case of Set 1, π^\pm and K^\pm are selected in the range $0.2 < p_T < 2.0$ GeV/c, while $p(\bar{p})$ is selected within $0.4 < p_T < 2.0$ GeV/c. In Set 2, $p(\bar{p})$, π^\pm , and K^\pm are restricted to the narrower range $0.4 < p_T < 1.6$ GeV/c. All measured diagonal and off-diagonal cumulants, κ_π^2 , κ_K^2 , κ_p^2 , $\kappa_{p,K}^{11}$, $\kappa_{\pi,K}^{11}$, $\kappa_{\pi,p}^{11}$, κ_Q^2 , $\kappa_{Q,K}^{11}$, and $\kappa_{Q,p}^{11}$, are shown in Fig. 1 for both sets. The observed centrality dependence is consistent with the fact that cumulants are extensive quantities, scaling proportionally to the system volume. The diagonal cumulants κ_π^2 , κ_K^2 , κ_p^2 , and κ_Q^2 , along with the off-diagonal cumulants $\kappa_{p,K}^{11}$, $\kappa_{\pi,K}^{11}$, and $\kappa_{\pi,p}^{11}$, show a dependence on the p_T interval. This behavior arises from the acceptance effect, where the chosen phase-space coverage influences the observed cumulant values [70]. On the other hand, $\kappa_{Q,K}^{11}$ and $\kappa_{Q,p}^{11}$ remain consistent within the uncertainties across the two p_T ranges, due to the interplay among their constituent terms: $\kappa_{Q,K}^{11} = \kappa_{p,K}^{11} + \kappa_{\pi,K}^{11} + \kappa_K^2$ and $\kappa_{Q,p}^{11} = \kappa_{p,K}^{11} + \kappa_{\pi,p}^{11} + \kappa_p^2$, leading to small variations.

To explore the underlying physics mechanisms, the measurements are compared with model predictions from HIJING [65], EPOS LHC [71], and Thermal-FIST (referred to as TheFIST in figures) [72], each offering a different approach to collision dynamics and hadronization. Resonance decays are included in all model calculations. The HIJING model (HIJING/ $B\bar{B}$ v2.0 [73]) treats nucleus–nucleus collisions as a superposition of independent binary collisions of wounded nucleons, incorporating phenomena such as baryon junctions, mini-jet production, parton shadowing, and jet quenching, while excluding effects like thermal equilibrium and collectivity. The EPOS LHC model, on the other hand, introduces collective effects through effective parton ladder splitting, separating the high-density central core from the peripheral corona. This model, a parametrized version of EPOS 1.99 [74], does not fully utilize the comprehensive 3D hydrodynamic calculation and subsequent hadronic cascade employed in the original EPOS framework. The HRG model of Thermal-FIST, employs a thermal-statistical approach to hadronization, and determines hadron abundances at the freeze-out of inelastic interactions based on derivatives of the system's partition function. The key parameters of the model, the chemical freeze-out temperature (T_{chem}), the volume corresponding to one unit of rapidity (dV/dy), and the strangeness saturation factor (γ_s) [75, 76], are tuned using the hadron yields measured by ALICE [77–80] for different centralities. The p_T spectra are modeled using blast-wave fits from Ref. [77]. This model functions within both the grand-canonical ensemble (GCE) and canonical ensemble (CE) frameworks. In the GCE, the electric charge, baryon number, and strangeness are conserved only on average across the entire system, whereas in the CE, these quantities are conserved exactly within a fixed volume (V_c) [81, 82]. The V_c , known as the correlation volume, is a defined region in phase space that ensures local conservation of QCD charges. In this approach, $V_c = kdV/dy$ implies that the system is truncated to k units around midrapidity, i.e., $|y| < k/2$, making it equivalent to a global conservation model with a reduced rapidity cut-off [83]. Therefore, in the V_c approach, the size and geometry of the correlation volume impose certain limitations on fluctuation observables. For example, this approach provides accurate results for rapidities $|y_{\text{cut}}| \lesssim k/4$ when fluctuations are measured within $|y| < y_{\text{cut}}$, but fails at higher rapidities [83]. There are also alternative methods for modeling local conservation of charges, based on the correlation length between particle and antiparticle in rapidity space [29, 83, 84]. In this analysis, the V_c formula-

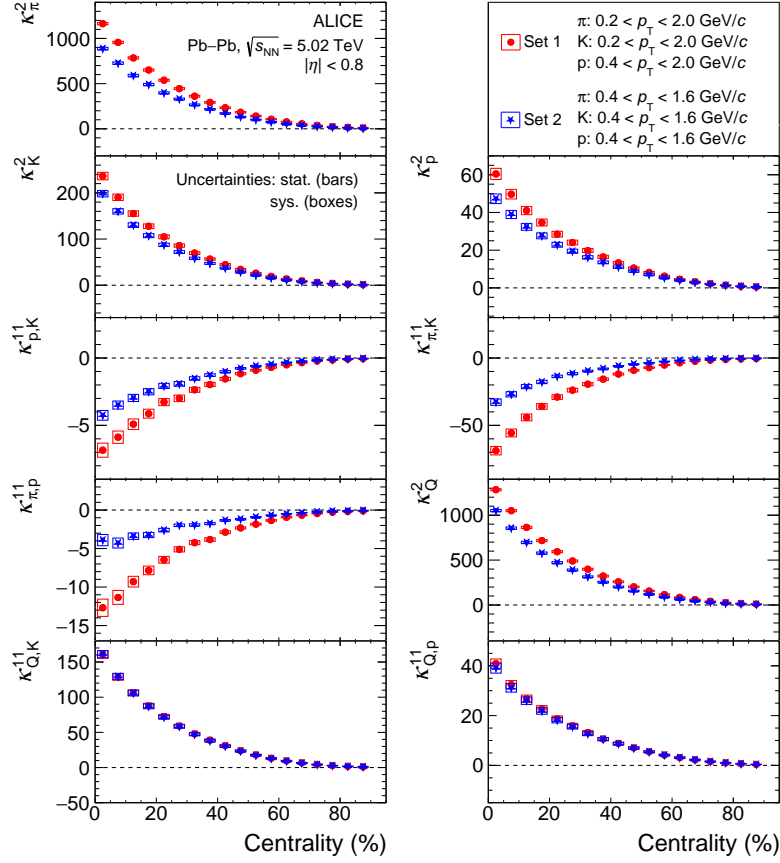


Figure 1: Centrality dependence of diagonal cumulants (κ_α^2) and off-diagonal cumulants ($\kappa_{\alpha,\beta}^{11}$) for the net-pion, net-kaon, net-proton, and net-charged particle distributions in Pb–Pb collisions at $\sqrt{s_{NN}} = 5.02$ TeV. The measurements are shown for two different p_T ranges. The statistical (systematic) uncertainties are represented by vertical bars (boxes).

tion is adopted, with V_c initially fixed to $3dV/dy$ for the CE calculations, following the parametrization in Ref. [82], which accurately describes the yield of light-flavored particles across all colliding systems with a precision better than 15%. The recent ALICE measurements of the second-order cumulants of net-proton, net- Ξ , and the correlation between net- Ξ and net-kaon are also described by the Thermal-FIST model with $V_c = 3dV/dy$, within experimental uncertainties [85].

The correlations $C_{Q,p}$, $C_{Q,K}$, and $C_{p,K}$ are shown in the top, middle, and bottom panels, respectively, in Fig. 2. The left column presents results obtained for Set 1 p_T acceptance, while the right column shows results for Set 2. All three correlations exhibit a weak centrality dependence, with $C_{p,K}$ following a trend opposite to that of $C_{Q,K}$ and $C_{Q,p}$. The deviation from the Poisson baseline (unity for $C_{Q,p}$ and $C_{Q,K}$, and zero for $C_{p,K}$) can be attributed to dynamic effects such as collectivity, resonance decays, and charge conservation [34, 35, 37, 38, 86].

The HIJING model expectations are closer to the data for $C_{Q,p}$ and $C_{Q,K}$, but fail to capture the observed trends and magnitudes, with significant discrepancies in $C_{p,K}$, mainly due to the incomplete modeling of resonance decays, which affect final-state interactions and the resulting particle correlations [65, 73]. HIJING remains constant with centrality, possibly due to the absence of collective dynamics, whereas the EPOS LHC model shows a visible centrality dependence driven by varying contributions from the "core" and "corona" regions. EPOS LHC captures the decreasing trend of $C_{p,K}$ with centrality, but predicts opposite trends for $C_{Q,p}$ and $C_{Q,K}$ compared to the data. The GCE results from Thermal-FIST model

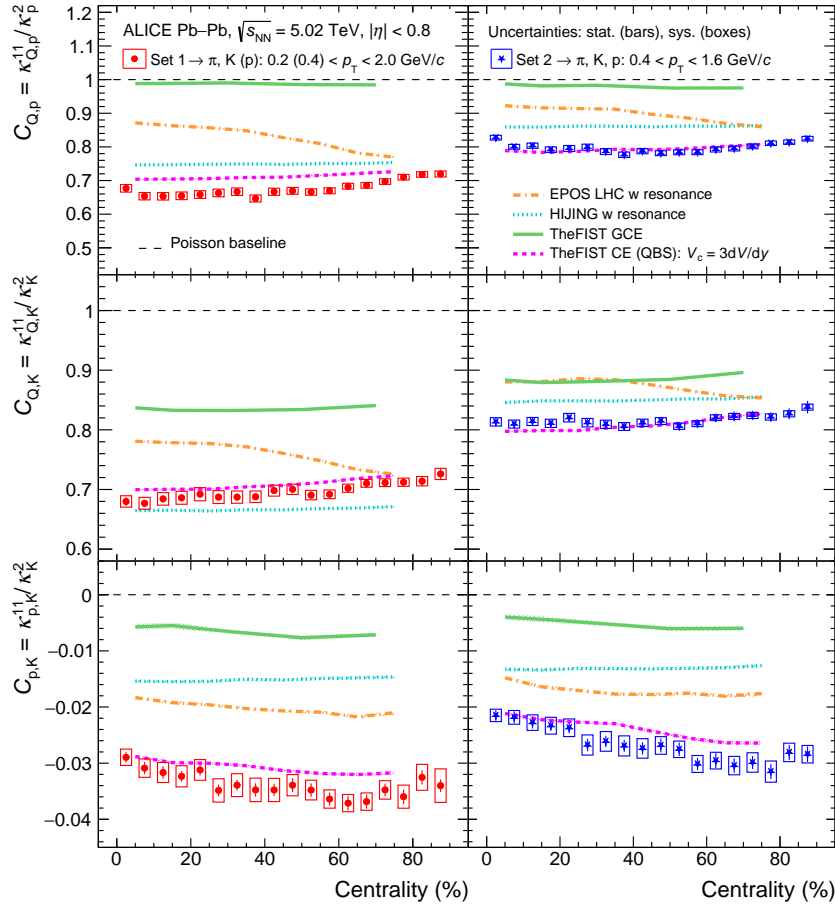


Figure 2: Centrality dependence of correlations $C_{Q,p}$ (top), $C_{Q,K}$ (middle), and $C_{p,K}$ (bottom) in Pb–Pb collisions at $\sqrt{s_{NN}} = 5.02$ TeV. The measurements are shown for two different p_T ranges in left and right columns. The predictions from HIJING [65], EPOS LHC [71], and Thermal-FIST (TheFIST) [72] model calculations with the grand canonical ensemble (GCE) and canonical ensemble (CE) formulation are denoted by colored lines. In the CE calculations, the electric charge (Q), baryon number (B), and strangeness (S) are conserved in a correlation volume of $V_c = 3dV/dy$. The statistical (systematic) uncertainties are represented by vertical bars (boxes), and the dashed line corresponds to the Poisson baseline.

completely fail to describe the measurements in both Set 1 and Set 2 p_T acceptances. At the same time, the CE calculations show better agreement with the data compared to all the other models discussed. It is seen that CE captures both the magnitude and centrality dependence of the correlations, particularly for the p_T acceptance in Set 2. This indicates that local conservation of charges in the CE formalism provides a more accurate explanation of the observed fluctuations and correlations in the experiment. However, further adjustments, such as varying V_c in the CE formalism, may improve the model’s agreement with the data.

In Fig. 3, the correlations, $C_{p,K}$, $C_{Q,p}$, and $C_{Q,K}$ for Set 1 p_T acceptance are compared with the Thermal-FIST results in the CE formalism, incorporating different V_c values. The model parameters, T_{chem} and γ_s are fixed to 155 MeV [87] and 1 [76], respectively, across all centralities, while V_c is systematically varied between $2dV/dy$ and $4dV/dy$. A quantitative comparison is performed by calculating the χ^2 values between the experimental data and model predictions for varying V_c , considering only the statistical uncertainties. To account for all three correlations, a combined χ^2 is defined as $\chi^2_{combined} = \chi^2_{C_{p,K}} + \chi^2_{C_{Q,p}} +$

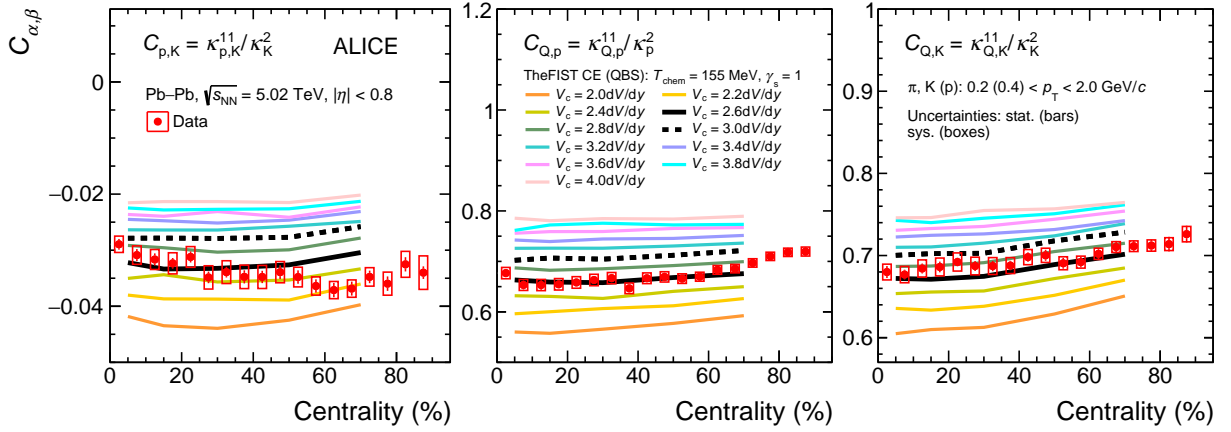


Figure 3: (Color online) Correlations $C_{p,K}$ (left), $C_{Q,p}$ (middle), and $C_{Q,K}$ (right) are shown as a function of centrality in Pb–Pb collisions at $\sqrt{s_{NN}} = 5.02$ TeV. Colored lines represent Thermal-FIST (TheFIST) [72] model calculations for the canonical ensemble (CE) with different correlation volumes (V_c). The statistical (systematic) uncertainties are represented by vertical bars (boxes).

$\chi^2_{C_{Q,K}}$. The best estimate of V_c is determined by minimizing χ^2_{combined} , with its statistical uncertainty calculated as half of the difference between the values of V_c in which $\chi^2_{\text{combined}} = \text{MIN}(\chi^2_{\text{combined}}) + 1$. Systematic uncertainties on $C_{p,K}$, $C_{Q,p}$, and $C_{Q,K}$ are taken into account in the evaluation of V_c . The combined χ^2 minimization is repeated after shifting the observables up and down by their respective systematic uncertainties, with half of the resulting difference assigned as the systematic uncertainty for V_c . The total uncertainty is then obtained by combining the statistical and systematic uncertainties in quadrature. This procedure yields $V_c = (2.60 \pm 0.11) \text{dV/dy}$ for the Set 1 and $V_c = (2.82 \pm 0.14) \text{dV/dy}$ for the Set 2 p_T acceptances. It is important to note that the extracted V_c values may be affected by the treatment of resonance decays in the Thermal-FIST model, as resonances play a significant role in shaping particle yields and their correlations.

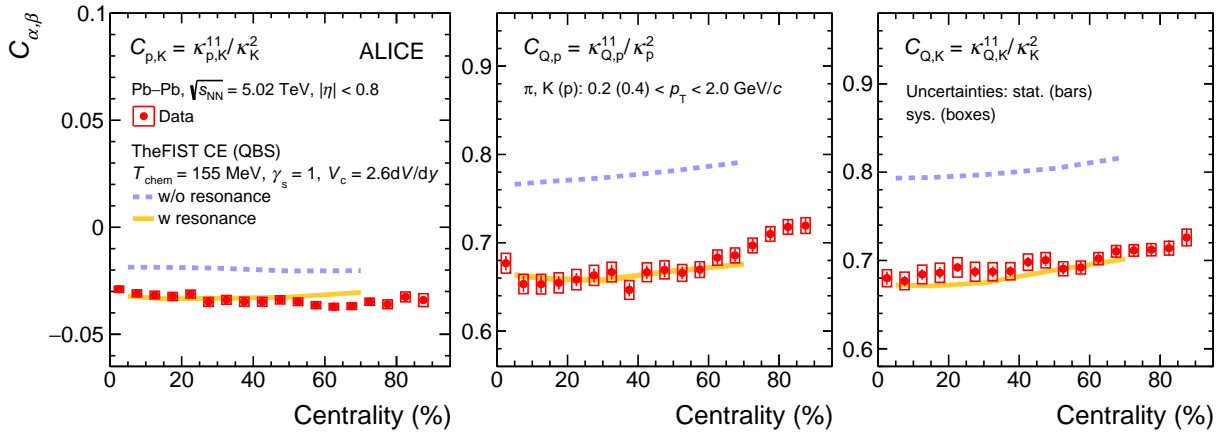


Figure 4: Correlations $C_{p,K}$ (left), $C_{Q,p}$ (middle), and $C_{Q,K}$ (right) are shown as a function of centrality in Pb–Pb collisions at $\sqrt{s_{NN}} = 5.02$ TeV. Colored lines represent Thermal-FIST (TheFIST) [72] model calculations for canonical ensemble (CE) with (w) and without (w/o) resonance contribution. The statistical (systematic) uncertainties are represented by vertical bars (boxes).

Figure 4 compares $C_{p,K}$, $C_{Q,p}$, and $C_{Q,K}$ for Set 1 p_T acceptance with Thermal-FIST CE calculations (using model parameters $T_{\text{chem}} = 155$ MeV, $\gamma_s = 1$, and $V_c = 2.6 \text{dV/dy}$), both with and without the

contribution of resonance decays. Including resonance decays in the model significantly enhances correlations across all centralities, accurately describing all three correlations, while excluding them fails to reproduce the observed results. The influence of resonances on the normalized second-order cumulants of net-pions and net-kaons has also been studied previously using the HIJING model in Ref. [29].

One can also study the ratios of the off-diagonal cumulants $\kappa_{Q,p}^{11}$ and $\kappa_{Q,K}^{11}$, to the diagonal cumulant κ_Q^2 to eliminate the dependence on V_c . In these ratios, the V_c dependence cancels out due to the same linear dependence on the acceptance fraction α_{acc} of both the numerator and the denominator [43]. The measurements of $\kappa_{Q,p}^{11}/\kappa_Q^2$ and $\kappa_{Q,K}^{11}/\kappa_Q^2$ for Set 1 p_T interval, compared with model results, are shown in the left and right panels of Fig. 5, respectively. The Thermal-FIST model results with different V_c values are comparable despite small deviations, which can be attributed to the imperfect cancelation of the acceptance factor (the net-charged particle is defined as the sum of the net-pion, net-kaon, and net-proton) and the specific implementation of V_c in the model [83]. The model could not fully capture the centrality dependence of the data, and overestimates its magnitude. This discrepancy could be due to an incomplete description of the resonance decays, assumptions in the V_c approach, or missing effects such as initial-state fluctuations and final-state interactions.

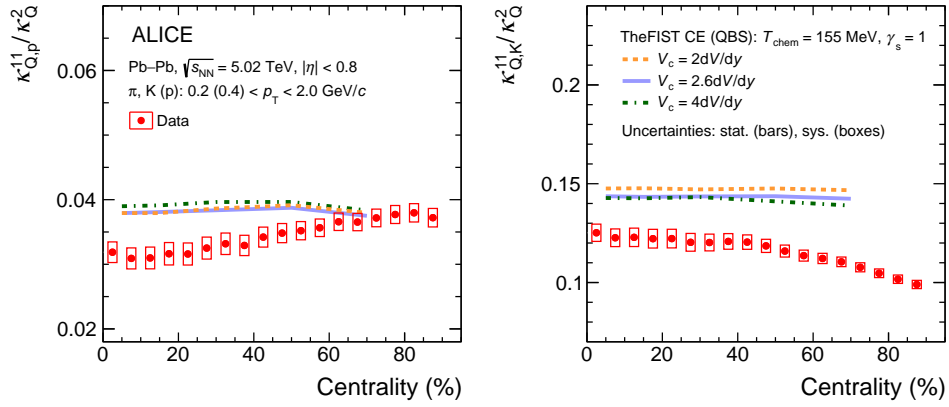


Figure 5: Centrality dependence of $\kappa_{Q,p}^{11}/\kappa_Q^2$ (left) and $\kappa_{Q,K}^{11}/\kappa_Q^2$ (right) in Pb–Pb collisions at $\sqrt{s_{\text{NN}}} = 5.02$ TeV. Colored lines represent Thermal-FIST (TheFIST) [72] model calculations for canonical ensemble (CE) with different correlation volumes (V_c). The statistical (systematic) uncertainties are represented by vertical bars (boxes).

Another possible factor affecting the cumulants and their ratios is the initial magnetic field generated by the spectator protons [51, 52]. Figure 6 shows the centrality dependence of $(2\kappa_{Q,K}^{11} - \kappa_{p,K}^{11})/\kappa_K^2$ and $(2\kappa_{Q,p}^{11} - \kappa_{p,K}^{11})/\kappa_p^2$, which have been proposed as observables sensitive to the magnetic field [51]. Both measurements exhibit a subtle increase from semi-central to peripheral collisions. The ratio $(2\kappa_{Q,K}^{11} - \kappa_{p,K}^{11})/\kappa_K^2$ rises by $\sim 4\%$ from the 50–55% to 85–90% centrality class, while $(2\kappa_{Q,p}^{11} - \kappa_{p,K}^{11})/\kappa_p^2$ increases by $\sim 5\%$, with relative significances of 2.1σ and 2.8σ , respectively. Despite the absence of the magnetic field effect in the model, the Thermal-FIST CE calculations describe the measurements within experimental uncertainties. While these ratios do not show a clear signature of the magnetic field, the scaled ratio $(\kappa_{Q,p}^{11}/\kappa_Q^2)/(\kappa_{Q,p}^{11}/\kappa_Q^2)^{0-5\%}$ exhibits a more pronounced centrality dependence, as shown in Fig. 7. For both Set 1 (left) and Set 2 (right), this ratio increases with centrality, following a trend consistent with LQCD predictions [52]. In Set 1, the observable deviates from unity beyond 40% centrality, increasing by nearly 20% at 85–90% centrality, while in Set 2, the deviation starts at 25% centrality and reaches almost 50% at 85–90% centrality. The measurements are compared to Thermal-FIST CE calculations without magnetic field for V_c values of 2.6dV/dy, 2.8dV/dy and 3.0dV/dy, with model results consistent across these V_c values. The model fails to explain the deviation beyond 50% centrality, which could result from incomplete resonance decay descriptions, missing physical processes, or possibly an influence from the initial magnetic field. Further investigation is required to confirm whether a magnetic

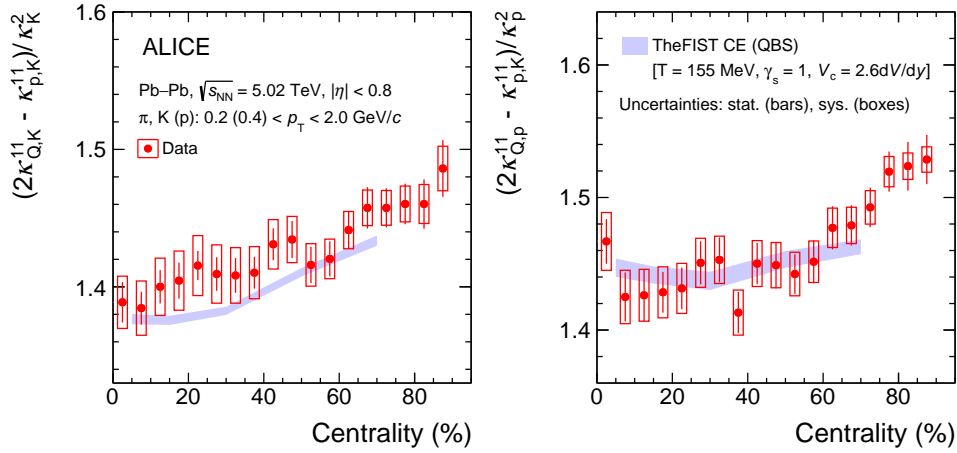


Figure 6: Centrality dependence of $(2\kappa_{Q,K}^{11} - \kappa_{p,K}^{11})/\kappa_K^2$ (left) and $(2\kappa_{Q,p}^{11} - \kappa_{p,K}^{11})/\kappa_p^2$ (right) in Pb–Pb collisions at $\sqrt{s_{NN}} = 5.02$ TeV. Thermal-FIST (TheFIST) [72] model calculation for canonical ensemble (CE) with a correlation volume of $V_c = 2.6dV/dy$ is represented by the colored band. The statistical (systematic) uncertainties are represented by vertical bars (boxes).

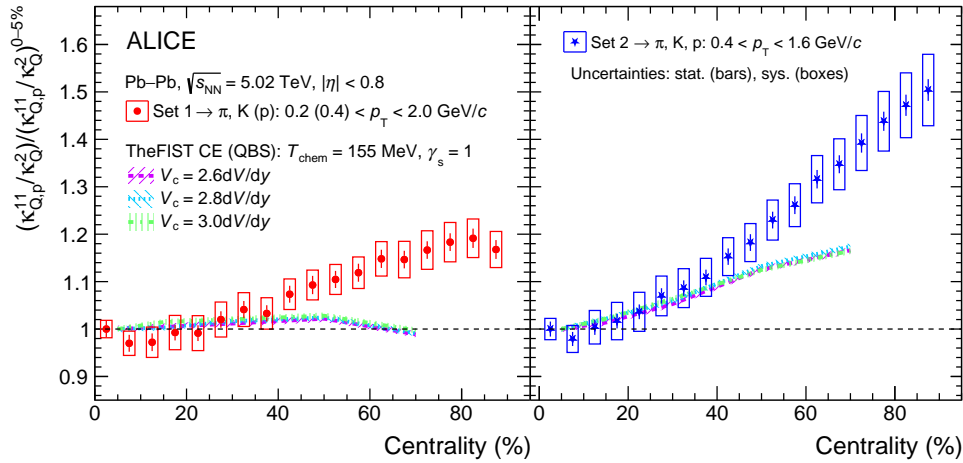


Figure 7: Centrality dependence of $(\kappa_{Q,p}^{11}/\kappa_Q^2)/(\kappa_{Q,p}^{11}/\kappa_Q^2)^{0.5\%}$ in Pb–Pb collisions at $\sqrt{s_{NN}} = 5.02$ TeV for Set 1 (left) and Set 2 (right) p_T acceptances. The colored bands represent the Thermal-FIST (TheFIST) [72] model calculations for canonical ensemble (CE) with different V_c values. The statistical (systematic) uncertainties are represented by vertical bars (boxes).

field effect contributes to these trends or if other factors dominate.

Figure 8 shows $C_{p,K}$, $C_{Q,p}$, and $C_{Q,K}$ as a function of collision energy for central and peripheral events, combining ALICE data at $\sqrt{s_{NN}} = 5.02$ TeV for Pb–Pb collisions and STAR data for Au+Au collisions from $\sqrt{s_{NN}} = 7.7 - 200$ GeV [31]. While the STAR results correspond to $|\eta| < 0.5$, the ALICE measurements are presented for both $|\eta| < 0.5$ and $|\eta| < 0.8$, offering insights into the effect of increasing acceptance window. All three correlations exhibit a monotonic decrease from RHIC to LHC energies. Notably, the deviation from the Poisson baseline increases with energy for both central and peripheral events, which is due to several differences in the underlying physics processes. A key factor is the decreasing beam rapidity with decreasing energy, which leads to a higher number of stopped protons in the kinematic acceptance and an increase in the α_{acc} — both crucial for the description of global and local charge conservation. In addition, volume fluctuations, which cannot be completely suppressed even in

narrow centrality bins, may contribute to the observed trend.

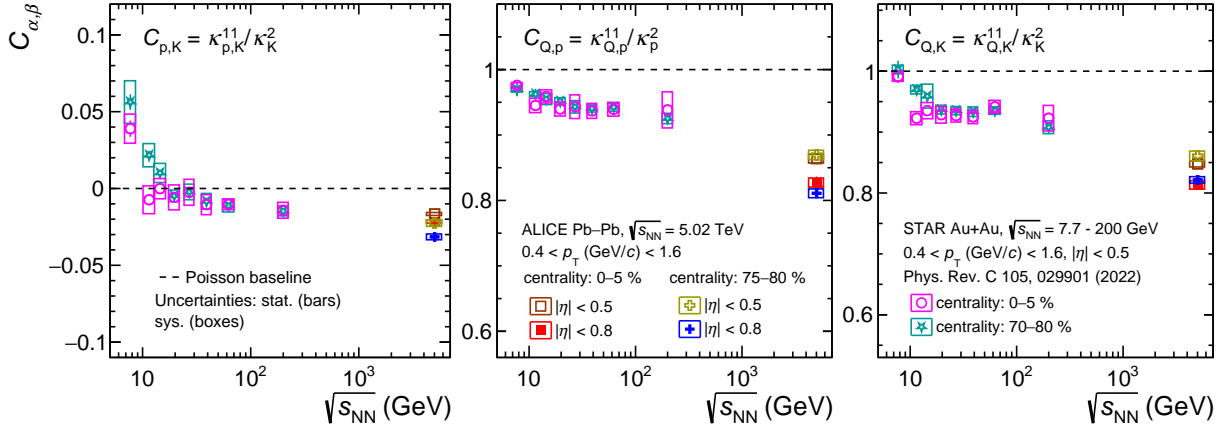


Figure 8: Energy dependence of $C_{p,K}$ (left), $C_{Q,p}$ (middle), and $C_{Q,K}$ (right), with lower energy results corresponding to STAR experiment [31]. The statistical (systematic) uncertainties are represented by vertical bars (boxes) and the dashed line corresponds to Poisson baseline.

4 Summary

This letter presents the centrality dependence of correlations among the net-charged particle, net-proton, and net-kaon ($C_{p,K}$, $C_{Q,p}$, and $C_{Q,K}$) measured in Pb–Pb collisions at $\sqrt{s_{NN}} = 5.02$ TeV, with net-proton and net-kaon serving as proxies for the net-baryon and the net-strangeness. All three correlations show pronounced deviations from the Poisson baseline, with resonance decays and charge conservation being significant contributing effects. Model calculations from HIJING, EPOS LHC, and Thermal-FIST in the grand canonical ensemble fail to explain the measurements. However, the Thermal-FIST model in the canonical ensemble, based on local charge conservation of the electric charge, baryon number, and strangeness, exhibits a better agreement with the data across all centralities. A combined χ^2 analysis of the correlations yields estimates of the correlation volume as $(2.60 \pm 0.11)dV/dy$ for the p_T range $0.2 < p_T < 2.0$ GeV/ c , and $(2.82 \pm 0.14)dV/dy$ for $0.4 < p_T < 1.6$ GeV/ c . The obtained correlation volumes — a specific implementation of the Thermal-FIST model — may be influenced by an incomplete implementation of resonance decays, assumptions in the V_c approach, or missing dynamical effects such as initial-state fluctuations and final-state interactions. The ratios $\kappa_{Q,p}^{11}/\kappa_Q^2$ and $\kappa_{Q,K}^{11}/\kappa_Q^2$, which are independent from the choice of V_c , reveal a notable deviation from the Thermal-FIST model calculations, which underscores the need for a better understanding of the underlying physics processes. Lattice QCD calculations predict that specific combinations of susceptibilities for the electric charge, baryon number, and strangeness are sensitive to the magnetic field, and these are studied experimentally using their corresponding proxies. While $(2\kappa_{Q,K}^{11} - \kappa_{p,K}^{11})/\kappa_K^2$ and $(2\kappa_{Q,p}^{11} - \kappa_{p,K}^{11})/\kappa_p^2$ display a subtle increase from semicentral to peripheral collisions, the scaled ratio $(\kappa_{Q,p}^{11}/\kappa_Q^2)/(\kappa_{Q,p}^{11}/\kappa_Q^2)^{0-5\%}$ shows a more pronounced increase, in qualitative agreement with LQCD predictions. Thermal-FIST calculations without magnetic field fail to reproduce the observed trend beyond 50% centrality, indicating the need for further investigations to confirm the magnetic field effect and rule out other possible explanations. The collision energy dependence of $C_{p,K}$, $C_{Q,p}$, and $C_{Q,K}$ shows a decrease from RHIC to LHC energies, with larger deviations from the Poisson baseline at higher energies. Understanding the impact of physics mechanisms such as stopped protons and changes in beam rapidity, is crucial for accurately modeling global and local charge conservation and correcting for volume fluctuations.

Acknowledgements

The ALICE Collaboration would like to thank all its engineers and technicians for their invaluable contributions to the construction of the experiment and the CERN accelerator teams for the outstanding performance of the LHC complex. The ALICE Collaboration gratefully acknowledges the resources and support provided by all Grid centres and the Worldwide LHC Computing Grid (WLCG) collaboration. The ALICE Collaboration acknowledges the following funding agencies for their support in building and running the ALICE detector: A. I. Alikhanyan National Science Laboratory (Yerevan Physics Institute) Foundation (ANSL), State Committee of Science and World Federation of Scientists (WFS), Armenia; Austrian Academy of Sciences, Austrian Science Fund (FWF): [M 2467-N36] and Nationalstiftung für Forschung, Technologie und Entwicklung, Austria; Ministry of Communications and High Technologies, National Nuclear Research Center, Azerbaijan; Conselho Nacional de Desenvolvimento Científico e Tecnológico (CNPq), Financiadora de Estudos e Projetos (Finep), Fundação de Amparo à Pesquisa do Estado de São Paulo (FAPESP) and Universidade Federal do Rio Grande do Sul (UFRGS), Brazil; Bulgarian Ministry of Education and Science, within the National Roadmap for Research Infrastructures 2020-2027 (object CERN), Bulgaria; Ministry of Education of China (MOEC), Ministry of Science & Technology of China (MSTC) and National Natural Science Foundation of China (NSFC), China; Ministry of Science and Education and Croatian Science Foundation, Croatia; Centro de Aplicaciones Tecnológicas y Desarrollo Nuclear (CEADEN), Cubaenergía, Cuba; Ministry of Education, Youth and Sports of the Czech Republic, Czech Republic; The Danish Council for Independent Research | Natural Sciences, the VILLUM FONDEN and Danish National Research Foundation (DNRF), Denmark; Helsinki Institute of Physics (HIP), Finland; Commissariat à l’Energie Atomique (CEA) and Institut National de Physique Nucléaire et de Physique des Particules (IN2P3) and Centre National de la Recherche Scientifique (CNRS), France; Bundesministerium für Bildung und Forschung (BMBF) and GSI Helmholtzzentrum für Schwerionenforschung GmbH, Germany; General Secretariat for Research and Technology, Ministry of Education, Research and Religions, Greece; National Research, Development and Innovation Office, Hungary; Department of Atomic Energy Government of India (DAE), Department of Science and Technology, Government of India (DST), University Grants Commission, Government of India (UGC) and Council of Scientific and Industrial Research (CSIR), India; National Research and Innovation Agency - BRIN, Indonesia; Istituto Nazionale di Fisica Nucleare (INFN), Italy; Japanese Ministry of Education, Culture, Sports, Science and Technology (MEXT) and Japan Society for the Promotion of Science (JSPS) KAKENHI, Japan; Consejo Nacional de Ciencia (CONACYT) y Tecnología, through Fondo de Cooperación Internacional en Ciencia y Tecnología (FONCICYT) and Dirección General de Asuntos del Personal Académico (DGAPA), Mexico; Nederlandse Organisatie voor Wetenschappelijk Onderzoek (NWO), Netherlands; The Research Council of Norway, Norway; Pontificia Universidad Católica del Perú, Peru; Ministry of Science and Higher Education, National Science Centre and WUT ID-UB, Poland; Korea Institute of Science and Technology Information and National Research Foundation of Korea (NRF), Republic of Korea; Ministry of Education and Scientific Research, Institute of Atomic Physics, Ministry of Research and Innovation and Institute of Atomic Physics and Universitatea Nationala de Stiinta si Tehnologie Politehnica Bucuresti, Romania; Ministerstvo školstva, vyzkumu, vyvoja a mladeze SR, Slovakia; National Research Foundation of South Africa, South Africa; Swedish Research Council (VR) and Knut & Alice Wallenberg Foundation (KAW), Sweden; European Organization for Nuclear Research, Switzerland; Suranaree University of Technology (SUT), National Science and Technology Development Agency (NSTDA) and National Science, Research and Innovation Fund (NSRF via PMU-B B05F650021), Thailand; Turkish Energy, Nuclear and Mineral Research Agency (TENMAK), Turkey; National Academy of Sciences of Ukraine, Ukraine; Science and Technology Facilities Council (STFC), United Kingdom; National Science Foundation of the United States of America (NSF) and United States Department of Energy, Office of Nuclear Physics (DOE NP), United States of America. In addition, individual groups or members have received support from: Czech Science Foundation (grant no. 23-07499S), Czech Republic; FORTE project, reg. no.

CZ.02.01.01/00/22_008/0004632, Czech Republic, co-funded by the European Union, Czech Republic; European Research Council (grant no. 950692), European Union; Deutsche Forschungs Gemeinschaft (DFG, German Research Foundation) “Neutrinos and Dark Matter in Astro- and Particle Physics” (grant no. SFB 1258), Germany; ICSC - National Research Center for High Performance Computing, Big Data and Quantum Computing and FAIR - Future Artificial Intelligence Research, funded by the NextGenerationEU program (Italy).

References

- [1] E. V. Shuryak, “Event per event analysis of heavy ion collisions and thermodynamical fluctuations”, *Phys. Lett. B* **423** (1998) 9–14, arXiv:hep-ph/9704456.
- [2] M. A. Stephanov, K. Rajagopal, and E. V. Shuryak, “Event-by-event fluctuations in heavy ion collisions and the QCD critical point”, *Phys. Rev. D* **60** (1999) 114028, arXiv:hep-ph/9903292.
- [3] H. Heiselberg, “Event-by-event physics in relativistic heavy ion collisions”, *Phys. Rept.* **351** (2001) 161–194, arXiv:nucl-th/0003046.
- [4] ALICE Collaboration, S. Acharya *et al.*, “The ALICE experiment: a journey through QCD”, *Eur. Phys. J. C* **84** (2024) 813, arXiv:2211.04384 [nucl-ex].
- [5] V. Koch, A. Majumder, and J. Randrup, “Baryon-strangeness correlations: A Diagnostic of strongly interacting matter”, *Phys. Rev. Lett.* **95** (2005) 182301, arXiv:nucl-th/0505052.
- [6] R. V. Gavai and S. Gupta, “Fluctuations, strangeness and quasi-quarks in heavy-ion collisions from lattice QCD”, *Phys. Rev. D* **73** (2006) 014004, arXiv:hep-lat/0510044.
- [7] M. Bluhm and B. Kampfer, “Flavor Diagonal and Off-Diagonal Susceptibilities in a Quasiparticle Model of the Quark-Gluon Plasma”, *Phys. Rev. D* **77** (2008) 114016, arXiv:0801.4147 [hep-ph].
- [8] A. Hietanen and K. Rummukainen, “The Diagonal and off-diagonal quark number susceptibility of high temperature and finite density QCD”, *JHEP* **04** (2008) 078, arXiv:0802.3979 [hep-lat].
- [9] S. Gupta, X. Luo, B. Mohanty, H. G. Ritter, and N. Xu, “Scale for the Phase Diagram of Quantum Chromodynamics”, *Science* **332** (2011) 1525–1528, arXiv:1105.3934 [hep-ph].
- [10] HotQCD Collaboration, A. Bazavov *et al.*, “Fluctuations and Correlations of net baryon number, electric charge, and strangeness: A comparison of lattice QCD results with the hadron resonance gas model”, *Phys. Rev. D* **86** (2012) 034509, arXiv:1203.0784 [hep-lat].
- [11] H.-T. Ding, F. Karsch, and S. Mukherjee, “Thermodynamics of strong-interaction matter from Lattice QCD”, *Int. J. Mod. Phys. E* **24** (2015) 1530007, arXiv:1504.05274 [hep-lat].
- [12] HotQCD Collaboration, H. T. Ding *et al.*, “Chiral Phase Transition Temperature in (2+1)-Flavor QCD”, *Phys. Rev. Lett.* **123** (2019) 062002, arXiv:1903.04801 [hep-lat].
- [13] S. Borsanyi, Z. Fodor, J. N. Guenther, S. K. Katz, K. K. Szabo, A. Pasztor, I. Portillo, and C. Ratti, “Higher order fluctuations and correlations of conserved charges from lattice QCD”, *JHEP* **10** (2018) 205, arXiv:1805.04445 [hep-lat].
- [14] ALICE Collaboration, S. Acharya *et al.*, “Measurements of Chemical Potentials in Pb-Pb Collisions at $\sqrt{s_{NN}}=5.02$ TeV”, *Phys. Rev. Lett.* **133** (2024) 092301, arXiv:2311.13332 [nucl-ex].

- [15] Y. Aoki, G. Endrodi, Z. Fodor, S. D. Katz, and K. K. Szabo, “The Order of the quantum chromodynamics transition predicted by the standard model of particle physics”, *Nature* **443** (2006) 675–678, arXiv:hep-lat/0611014.
- [16] S. Ejiri, “Canonical partition function and finite density phase transition in lattice QCD”, *Phys. Rev. D* **78** (2008) 074507, arXiv:0804.3227 [hep-lat].
- [17] J. Berges, D.-U. Jungnickel, and C. Wetterich, “The Chiral phase transition at high baryon density from nonperturbative flow equations”, *Eur. Phys. J. C* **13** (2000) 323–329, arXiv:hep-ph/9811347.
- [18] M. Asakawa and K. Yazaki, “Chiral Restoration at Finite Density and Temperature”, *Nucl. Phys. A* **504** (1989) 668–684.
- [19] M. A. Stephanov, “QCD phase diagram: An Overview”, *PoS LAT2006* (2006) 024, arXiv:hep-lat/0701002.
- [20] M. A. Stephanov, “Non-Gaussian fluctuations near the QCD critical point”, *Phys. Rev. Lett.* **102** (2009) 032301, arXiv:0809.3450 [hep-ph].
- [21] M. Asakawa, S. Ejiri, and M. Kitazawa, “Third moments of conserved charges as probes of QCD phase structure”, *Phys. Rev. Lett.* **103** (2009) 262301, arXiv:0904.2089 [nucl-th].
- [22] M. A. Stephanov, “On the sign of kurtosis near the QCD critical point”, *Phys. Rev. Lett.* **107** (2011) 052301, arXiv:1104.1627 [hep-ph].
- [23] F. Karsch and K. Redlich, “Probing freeze-out conditions in heavy ion collisions with moments of charge fluctuations”, *Phys. Lett. B* **695** (2011) 136–142, arXiv:1007.2581 [hep-ph].
- [24] B. Friman, F. Karsch, K. Redlich, and V. Skokov, “Fluctuations as probe of the QCD phase transition and freeze-out in heavy ion collisions at LHC and RHIC”, *Eur. Phys. J. C* **71** (2011) 1694, arXiv:1103.3511 [hep-ph].
- [25] **STAR** Collaboration, J. Adam *et al.*, “Nonmonotonic Energy Dependence of Net-Proton Number Fluctuations”, *Phys. Rev. Lett.* **126** (2021) 092301, arXiv:2001.02852 [nucl-ex].
- [26] **STAR** Collaboration, L. Adamczyk *et al.*, “Collision Energy Dependence of Moments of Net-Kaon Multiplicity Distributions at RHIC”, *Phys. Lett. B* **785** (2018) 551–560, arXiv:1709.00773 [nucl-ex].
- [27] X. Luo and N. Xu, “Search for the QCD Critical Point with Fluctuations of Conserved Quantities in Relativistic Heavy-Ion Collisions at RHIC : An Overview”, *Nucl. Sci. Tech.* **28** (2017) 112, arXiv:1701.02105 [nucl-ex].
- [28] A. Panday, D. Mallick, and B. Mohanty, “Search for the QCD critical point in high energy nuclear collisions”, *Prog. Part. Nucl. Phys.* **125** (2022) 103960, arXiv:2203.07817 [nucl-ex].
- [29] **ALICE** Collaboration, S. Acharya *et al.*, “Closing in on critical net-baryon fluctuations at LHC energies: Cumulants up to third order in Pb–Pb collisions”, *Phys. Lett. B* **844** (2023) 137545, arXiv:2206.03343 [nucl-ex].
- [30] R. Bellwied, S. Borsanyi, Z. Fodor, J. N. Guenther, J. Noronha-Hostler, P. Parotto, A. Pasztor, C. Ratti, and J. M. Stafford, “Off-diagonal correlators of conserved charges from lattice QCD and how to relate them to experiment”, *Phys. Rev. D* **101** (2020) 034506, arXiv:1910.14592 [hep-lat].

- [31] **STAR** Collaboration, J. Adam *et al.*, “Collision-energy dependence of second-order off-diagonal and diagonal cumulants of net-charge, net-proton, and net-kaon multiplicity distributions in Au + Au collisions”, *Phys. Rev. C* **100** (2019) 014902, arXiv:1903.05370 [nucl-ex]. [Erratum: *Phys.Rev.C* 105, 029901 (2022)].
- [32] **ALICE** Collaboration, J. Adam *et al.*, “Multiplicity and transverse momentum evolution of charge-dependent correlations in pp, p–Pb, and Pb–Pb collisions at the LHC”, *Eur. Phys. J. C* **76** (2016) 86, arXiv:1509.07255 [nucl-ex].
- [33] **ALICE** Collaboration, S. Acharya *et al.*, “General balance functions of identified charged hadron pairs of (π ,K,p) in Pb–Pb collisions at $\sqrt{s_{NN}}=2.76$ TeV”, *Phys. Lett. B* **833** (2022) 137338, arXiv:2110.06566 [nucl-ex].
- [34] V. Vovchenko and V. Koch, “Particlization of an interacting hadron resonance gas with global conservation laws for event-by-event fluctuations in heavy-ion collisions”, *Phys. Rev. C* **103** (2021) 044903, arXiv:2012.09954 [hep-ph].
- [35] P. Braun-Munzinger, A. Rustamov, and J. Stachel, “The role of the local conservation laws in fluctuations of conserved charges”, arXiv:1907.03032 [nucl-th].
- [36] P. Braun-Munzinger, A. Rustamov, and J. Stachel, “Bridging the gap between event-by-event fluctuation measurements and theory predictions in relativistic nuclear collisions”, *Nucl. Phys. A* **960** (2017) 114–130, arXiv:1612.00702 [nucl-th].
- [37] M. Bluhm *et al.*, “Dynamics of critical fluctuations: Theory – phenomenology – heavy-ion collisions”, *Nucl. Phys. A* **1003** (2020) 122016, arXiv:2001.08831 [nucl-th].
- [38] D. K. Mishra, P. Garg, P. K. Netrakanti, and A. K. Mohanty, “Effect of resonance decay on conserved number fluctuations in a hadron resonance gas model”, *Phys. Rev. C* **94** (2016) 014905, arXiv:1607.01875 [hep-ph].
- [39] C. Shen and B. Schenke, “Dynamical initial state model for relativistic heavy-ion collisions”, *Phys. Rev. C* **97** (2018) 024907, arXiv:1710.00881 [nucl-th].
- [40] Y. Ohnishi, M. Kitazawa, and M. Asakawa, “Thermal blurring of event-by-event fluctuations generated by rapidity conversion”, *Phys. Rev. C* **94** (2016) 044905, arXiv:1606.03827 [nucl-th].
- [41] A. Bzdak, V. Koch, and V. Skokov, “Baryon number conservation and the cumulants of the net proton distribution”, *Phys. Rev. C* **87** (2013) 014901, arXiv:1203.4529 [hep-ph].
- [42] V. Vovchenko, O. Savchuk, R. V. Poberezhnyuk, M. I. Gorenstein, and V. Koch, “Connecting fluctuation measurements in heavy-ion collisions with the grand-canonical susceptibilities”, *Phys. Lett. B* **811** (2020) 135868, arXiv:2003.13905 [hep-ph].
- [43] V. Vovchenko, R. V. Poberezhnyuk, and V. Koch, “Cumulants of multiple conserved charges and global conservation laws”, *JHEP* **10** (2020) 089, arXiv:2007.03850 [hep-ph].
- [44] **WA98** Collaboration, M. M. Aggarwal *et al.*, “Scaling of particle and transverse energy production in Pb-208 + Pb-208 collisions at 158-A-GeV”, *Eur. Phys. J. C* **18** (2001) 651–663, arXiv:nucl-ex/0008004.
- [45] A. Bialas, M. Bleszynski, and W. Czyz, “Multiplicity Distributions in Nucleus-Nucleus Collisions at High-Energies”, *Nucl. Phys. B* **111** (1976) 461–476.

- [46] V. Skokov, A. Y. Illarionov, and V. Toneev, “Estimate of the magnetic field strength in heavy-ion collisions”, *Int. J. Mod. Phys. A* **24** (2009) 5925–5932, arXiv:0907.1396 [nucl-th].
- [47] D. E. Kharzeev, L. D. McLerran, and H. J. Warringa, “The Effects of topological charge change in heavy ion collisions: ‘Event by event P and CP violation’”, *Nucl. Phys. A* **803** (2008) 227–253, arXiv:0711.0950 [hep-ph].
- [48] V. Voronyuk, V. D. Toneev, W. Cassing, E. L. Bratkovskaya, V. P. Konchakovski, and S. A. Voloshin, “(Electro-)Magnetic field evolution in relativistic heavy-ion collisions”, *Phys. Rev. C* **83** (2011) 054911, arXiv:1103.4239 [nucl-th].
- [49] R. K. Mohapatra, P. S. Saumia, and A. M. Srivastava, “Enhancement of flow anisotropies due to magnetic field in relativistic heavy-ion collisions”, *Mod. Phys. Lett. A* **26** (2011) 2477–2486, arXiv:1102.3819 [hep-ph].
- [50] K. Tuchin, “Photon decay in strong magnetic field in heavy-ion collisions”, *Phys. Rev. C* **83** (2011) 017901, arXiv:1008.1604 [nucl-th].
- [51] H. T. Ding, S. T. Li, Q. Shi, and X. D. Wang, “Fluctuations and correlations of net baryon number, electric charge and strangeness in a background magnetic field”, *Eur. Phys. J. A* **57** (2021) 202, arXiv:2104.06843 [hep-lat].
- [52] H.-T. Ding, J.-B. Gu, A. Kumar, S.-T. Li, and J.-H. Liu, “Baryon Electric Charge Correlation as a Magnetometer of QCD”, *Phys. Rev. Lett.* **132** (2024) 201903, arXiv:2312.08860 [hep-lat].
- [53] ALICE Collaboration, K. Aamodt *et al.*, “The ALICE experiment at the CERN LHC”, *JINST* **3** (2008) S08002.
- [54] ALICE Collaboration, B. B. Abelev *et al.*, “Performance of the ALICE Experiment at the CERN LHC”, *Int. J. Mod. Phys. A* **29** (2014) 1430044, arXiv:1402.4476 [nucl-ex].
- [55] ALICE Collaboration, K. Aamodt *et al.*, “Alignment of the ALICE Inner Tracking System with cosmic-ray tracks”, *JINST* **5** (2010) P03003, arXiv:1001.0502 [physics.ins-det].
- [56] J. Alme *et al.*, “The ALICE TPC, a large 3-dimensional tracking device with fast readout for ultra-high multiplicity events”, *Nucl. Instrum. Meth. A* **622** (2010) 316–367, arXiv:1001.1950 [physics.ins-det].
- [57] ALICE Collaboration, G. Dellacasa *et al.*, “ALICE technical design report of the time-of-flight system (TOF)”, *CERN-LHCC-2000-012* (2, 2000). <https://cds.cern.ch/record/545834>.
- [58] ALICE Collaboration, E. Abbas *et al.*, “Performance of the ALICE VZERO system”, *JINST* **8** (2013) P10016, arXiv:1306.3130 [nucl-ex].
- [59] ALICE Collaboration, P. Cortese *et al.*, “ALICE technical design report on forward detectors: FMD, T0 and V0”, *CERN-LHCC-2004-025* (9, 2004). <https://cds.cern.ch/record/781854>.
- [60] M. Arslanok, E. Hellbär, M. Ivanov, R. H. Münzer, and J. Wiechula, “Track Reconstruction in a High-Density Environment with ALICE”, *Particles* **5** (2022) 84–95, arXiv:2203.10325 [physics.ins-det].
- [61] ALICE Collaboration, B. Abelev *et al.*, “Centrality determination of Pb-Pb collisions at $\sqrt{s_{NN}} = 2.76$ TeV with ALICE”, *Phys. Rev. C* **88** (2013) 044909, arXiv:1301.4361 [nucl-ex].
- [62] ALICE Collaboration, B. Abelev *et al.*, “Centrality dependence of π , K, p production in Pb-Pb collisions at $\sqrt{s_{NN}} = 2.76$ TeV”, *Phys. Rev. C* **88** (2013) 044910, arXiv:1303.0737 [hep-ex].

- [63] T. Nonaka, M. Kitazawa, and S. Esumi, “More efficient formulas for efficiency correction of cumulants and effect of using averaged efficiency”, *Phys. Rev. C* **95** (2017) 064912, arXiv:1702.07106 [physics.data-an]. [Erratum: Phys.Rev.C 103, 029901 (2021)].
- [64] A. Bzdak and V. Koch, “Local Efficiency Corrections to Higher Order Cumulants”, *Phys. Rev. C* **91** (2015) 027901, arXiv:1312.4574 [nucl-th].
- [65] X.-N. Wang and M. Gyulassy, “HIJING: A Monte Carlo model for multiple jet production in p p, p A and A A collisions”, *Phys. Rev. D* **44** (1991) 3501–3516.
- [66] R. Brun, F. Bruyant, F. Carminati, S. Giani, M. Maire, A. McPherson, G. Patrick, and L. Urban, “GEANT Detector Description and Simulation Tool”, *CERN-W5013* (10, 1994). <http://cds.cern.ch/record/1082634>.
- [67] X. Luo and T. Nonaka, “Efficiency correction for cumulants of multiplicity distributions based on track-by-track efficiency”, *Phys. Rev. C* **99** (2019) 044917, arXiv:1812.10303 [physics.data-an].
- [68] X. Luo, “Unified description of efficiency correction and error estimation for moments of conserved quantities in heavy-ion collisions”, *Phys. Rev. C* **91** (2015) 034907, arXiv:1410.3914 [physics.data-an]. [Erratum: Phys.Rev.C 94, 059901 (2016)].
- [69] ALICE Collaboration, Archaya, S. and others, “Centrality determination in heavy ion collisions”, *ALICE-PUBLIC-2018-011* (8, 2018). <https://cds.cern.ch/record/2636623>.
- [70] B. Ling and M. A. Stephanov, “Acceptance dependence of fluctuation measures near the QCD critical point”, *Phys. Rev. C* **93** (2016) 034915, arXiv:1512.09125 [nucl-th].
- [71] T. Pierog, I. Karpenko, J. M. Katzy, E. Yatsenko, and K. Werner, “EPOS LHC: Test of collective hadronization with data measured at the CERN Large Hadron Collider”, *Phys. Rev. C* **92** (2015) 034906, arXiv:1306.0121 [hep-ph].
- [72] V. Vovchenko and H. Stoecker, “Thermal-FIST: A package for heavy-ion collisions and hadronic equation of state”, *Comput. Phys. Commun.* **244** (2019) 295–310, arXiv:1901.05249 [nucl-th].
- [73] V. Topor Pop, M. Gyulassy, J. Barrette, C. Gale, X. N. Wang, and N. Xu, “Baryon junction loops in HIJING / B anti-B v2.0 and the baryon /meson anomaly at RHIC”, *Phys. Rev. C* **70** (2004) 064906, arXiv:nucl-th/0407095.
- [74] T. Pierog and K. Werner, “EPOS Model and Ultra High Energy Cosmic Rays”, *Nucl. Phys. B Proc. Suppl.* **196** (2009) 102–105, arXiv:0905.1198 [hep-ph].
- [75] P. Koch, B. Muller, and J. Rafelski, “Strangeness in Relativistic Heavy Ion Collisions”, *Phys. Rept.* **142** (1986) 167–262.
- [76] J. Rafelski, “Strange anti-baryons from quark - gluon plasma”, *Phys. Lett. B* **262** (1991) 333–340.
- [77] ALICE Collaboration, S. Acharya *et al.*, “Production of charged pions, kaons, and (anti-)protons in Pb-Pb and inelastic *pp* collisions at $\sqrt{s_{NN}} = 5.02$ TeV”, *Phys. Rev. C* **101** (2020) 044907, arXiv:1910.07678 [nucl-ex].
- [78] ALICE Collaboration, B. B. Abelev *et al.*, “ $K^*(892)^0$ and $\phi(1020)$ production in Pb-Pb collisions at $\sqrt{s_{NN}} = 2.76$ TeV”, *Phys. Rev. C* **91** (2015) 024609, arXiv:1404.0495 [nucl-ex].

- [79] ALICE Collaboration, B. B. Abelev *et al.*, “ K_S^0 and Λ production in Pb-Pb collisions at $\sqrt{s_{NN}} = 2.76$ TeV”, *Phys. Rev. Lett.* **111** (2013) 222301, arXiv:1307.5530 [nucl-ex].
- [80] ALICE Collaboration, B. B. Abelev *et al.*, “Multi-strange baryon production at mid-rapidity in Pb-Pb collisions at $\sqrt{s_{NN}} = 2.76$ TeV”, *Phys. Lett. B* **728** (2014) 216–227, arXiv:1307.5543 [nucl-ex]. [Erratum: *Phys.Lett.B* 734, 409–410 (2014)].
- [81] F. Becattini, “An Introduction to the Statistical Hadronization Model”, in *International School on Quark-Gluon Plasma and Heavy Ion Collisions: past, present, future.* 1, 2009. arXiv:0901.3643 [hep-ph].
- [82] V. Vovchenko, B. Dönigus, and H. Stoecker, “Canonical statistical model analysis of p-p, p-Pb, and Pb-Pb collisions at energies available at the CERN Large Hadron Collider”, *Phys. Rev. C* **100** (2019) 054906, arXiv:1906.03145 [hep-ph].
- [83] V. Vovchenko, “Density correlations under global and local charge conservation”, *Phys. Rev. C* **110** (2024) L061902, arXiv:2409.01397 [hep-ph].
- [84] P. Braun-Munzinger, K. Redlich, A. Rustamov, and J. Stachel, “The imprint of conservation laws on correlated particle production”, *JHEP* **08** (2024) 113, arXiv:2312.15534 [nucl-th].
- [85] ALICE Collaboration, S. Acharya *et al.*, “Probing Strangeness Hadronization with Event-by-Event Production of Multistrange Hadrons”, *Phys. Rev. Lett.* **134** (2025) 022303, arXiv:2405.19890 [nucl-ex].
- [86] P. Garg, D. K. Mishra, P. K. Netrakanti, B. Mohanty, A. K. Mohanty, B. K. Singh, and N. Xu, “Conserved number fluctuations in a hadron resonance gas model”, *Phys. Lett. B* **726** (2013) 691–696, arXiv:1304.7133 [nucl-ex].
- [87] A. Andronic, P. Braun-Munzinger, K. Redlich, and J. Stachel, “Decoding the phase structure of QCD via particle production at high energy”, *Nature* **561** (2018) 321–330, arXiv:1710.09425 [nucl-th].

A The ALICE Collaboration

S. Acharya ⁵⁰, A. Agarwal¹³³, G. Aglieri Rinella ³², L. Aglietta ²⁴, M. Agnello ²⁹, N. Agrawal ²⁵, Z. Ahammed ¹³³, S. Ahmad ¹⁵, S.U. Ahn ⁷¹, I. Ahuja ³⁶, A. Akindinov ¹³⁹, V. Akishina³⁸, M. Al-Turany ⁹⁶, D. Aleksandrov ¹³⁹, B. Alessandro ⁵⁶, H.M. Alfanda ⁶, R. Alfaro Molina ⁶⁷, B. Ali ¹⁵, A. Alici ²⁵, N. Alizadehvandchali ¹¹⁴, A. Alkin ¹⁰³, J. Alme ²⁰, G. Alocco ²⁴, T. Alt ⁶⁴, A.R. Altamura ⁵⁰, I. Altsybeev ⁹⁴, J.R. Alvarado ⁴⁴, M.N. Anaam ⁶, C. Andrei ⁴⁵, N. Andreou ¹¹³, A. Andronic ¹²⁴, E. Andronov ¹³⁹, V. Anguelov ⁹³, F. Antinori ⁵⁴, P. Antonioli ⁵¹, N. Apadula ⁷³, H. Appelshäuser ⁶⁴, C. Arata ⁷², S. Arcelli ²⁵, R. Arnaldi ⁵⁶, J.G.M.C.A. Arneiro ¹⁰⁹, I.C. Arsene ¹⁹, M. Arslanok ¹³⁶, A. Augustinus ³², R. Averbeck ⁹⁶, D. Averyanov ¹³⁹, M.D. Azmi ¹⁵, H. Baba¹²², A. Badalà ⁵³, J. Bae ¹⁰³, Y. Bae ¹⁰³, Y.W. Baek ⁴⁰, X. Bai ¹¹⁸, R. Bailhache ⁶⁴, Y. Bailung ⁴⁸, R. Bala ⁹⁰, A. Baldisseri ¹²⁸, B. Balis ², S. Bangalia¹¹⁶, Z. Banoo ⁹⁰, V. Barbasova ³⁶, F. Barile ³¹, L. Barioglio ⁵⁶, M. Barlou ⁷⁷, B. Barman ⁴¹, G.G. Barnaföldi ⁴⁶, L.S. Barnby ¹¹³, E. Barreau ¹⁰², V. Barret ¹²⁵, L. Barreto ¹⁰⁹, K. Barth ³², E. Bartsch ⁶⁴, N. Bastid ¹²⁵, S. Basu ⁷⁴, G. Batigne ¹⁰², D. Battistini ⁹⁴, B. Batyunya ¹⁴⁰, D. Bauri⁴⁷, J.L. Bazo Alba ¹⁰⁰, I.G. Bearden ⁸², P. Becht ⁹⁶, D. Behera ⁴⁸, I. Belikov ¹²⁷, A.D.C. Bell Hechavarría ¹²⁴, F. Bellini ²⁵, R. Bellwied ¹¹⁴, S. Belokurova ¹³⁹, L.G.E. Beltran ¹⁰⁸, Y.A.V. Beltran ⁴⁴, G. Bencedi ⁴⁶, A. Bensaoula¹¹⁴, S. Beole ²⁴, Y. Berdnikov ¹³⁹, A. Berdnikova ⁹³, L. Bergmann ⁹³, L. Bernardinis²³, L. Betev ³², P.P. Bhaduri ¹³³, A. Bhasin ⁹⁰, B. Bhattacharjee ⁴¹, S. Bhattarai¹¹⁶, L. Bianchi ²⁴, J. Bielčik ³⁴, J. Bielčiková ⁸⁵, A.P. Bigot ¹²⁷, A. Bilandzic ⁹⁴, A. Binoy ¹¹⁶, G. Biro ⁴⁶, S. Biswas ⁴, N. Bize ¹⁰², D. Blau ¹³⁹, M.B. Blidaru ⁹⁶, N. Bluhme³⁸, C. Blume ⁶⁴, F. Bock ⁸⁶, T. Bodova ²⁰, J. Bok ¹⁶, L. Boldizsár ⁴⁶, M. Bombara ³⁶, P.M. Bond ³², G. Bonomi ^{132,55}, H. Borel ¹²⁸, A. Borissov ¹³⁹, A.G. Borquez Carcamo ⁹³, E. Botta ²⁴, Y.E.M. Bouziani ⁶⁴, D.C. Brandibur ⁶³, L. Bratrud ⁶⁴, P. Braun-Munzinger ⁹⁶, M. Bregant ¹⁰⁹, M. Broz ³⁴, G.E. Bruno ^{95,31}, V.D. Buchakchiev ³⁵, M.D. Buckland ⁸⁴, D. Budnikov ¹³⁹, H. Buesching ⁶⁴, S. Bufalino ²⁹, P. Buhler ¹⁰¹, N. Burmasov ¹³⁹, Z. Buthelezi ^{68,121}, A. Bylinkin ²⁰, S.A. Bysiak¹⁰⁶, J.C. Cabanillas Noris ¹⁰⁸, M.F.T. Cabrera ¹¹⁴, H. Caines ¹³⁶, A. Caliva ²⁸, E. Calvo Villar ¹⁰⁰, J.M.M. Camacho ¹⁰⁸, P. Camerini ²³, M.T. Camerlingo ⁵⁰, F.D.M. Canedo ¹⁰⁹, S. Cannito²³, S.L. Cantway ¹³⁶, M. Carabas ¹¹², F. Carnesecchi ³², L.A.D. Carvalho ¹⁰⁹, J. Castillo Castellanos ¹²⁸, M. Castoldi ³², F. Catalano ³², S. Cattaruzzi ²³, R. Cerri ²⁴, I. Chakaberia ⁷³, P. Chakraborty ¹³⁴, S. Chandra ¹³³, S. Chapeland ³², M. Chartier ¹¹⁷, S. Chattopadhyay¹³³, M. Chen ³⁹, T. Cheng ⁶, C. Cheshkov ¹²⁶, D. Chiappara ²⁷, V. Chibante Barroso ³², D.D. Chinellato ¹⁰¹, F. Chinu ²⁴, E.S. Chizzali ^{11,94}, J. Cho ⁵⁸, S. Cho ⁵⁸, P. Chochula ³², Z.A. Chochulska¹³⁴, D. Choudhury⁴¹, S. Choudhury⁹⁸, P. Christakoglou ⁸³, C.H. Christensen ⁸², P. Christiansen ⁷⁴, T. Chujo ¹²³, M. Ciaccio ²⁹, C. Cicalo ⁵², G. Cimador ²⁴, F. Cindolo ⁵¹, M.R. Ciupek⁹⁶, G. Clai^{III,51}, F. Colamaria ⁵⁰, J.S. Colburn⁹⁹, D. Colella ³¹, A. Colelli³¹, M. Colocci ²⁵, M. Concas ³², G. Conesa Balbastre ⁷², Z. Conesa del Valle ¹²⁹, G. Contin ²³, J.G. Contreras ³⁴, M.L. Coquet ¹⁰², P. Cortese ^{131,56}, M.R. Cosentino ¹¹¹, F. Costa ³², S. Costanza ²¹, P. Crochet ¹²⁵, M.M. Czarnynoga¹³⁴, A. Dainese ⁵⁴, G. Dange³⁸, M.C. Danisch ⁹³, A. Danu ⁶³, P. Das ³², S. Das ⁴, A.R. Dash ¹²⁴, S. Dash ⁴⁷, A. De Caro ²⁸, G. de Cataldo ⁵⁰, J. de Cuveland ³⁸, A. De Falco ²², D. De Gruttola ²⁸, N. De Marco ⁵⁶, C. De Martin ²³, S. De Pasquale ²⁸, R. Deb ¹³², R. Del Grande ⁹⁴, L. Dello Stritto ³², K.C. Devereaux¹⁸, G.G.A. de Souza ^{IV,109}, P. Dhankher ¹⁸, D. Di Bari ³¹, M. Di Costanzo ²⁹, A. Di Mauro ³², B. Di Ruzza ¹³⁰, B. Diab ³², R.A. Diaz ¹⁴⁰, Y. Ding ⁶, J. Ditzel ⁶⁴, R. Divià ³², Ø. Djuvsland²⁰, U. Dmitrieva ¹³⁹, A. Dobrin ⁶³, B. Dönigus ⁶⁴, J.M. Dubinski ¹³⁴, A. Dubla ⁹⁶, P. Dupieux ¹²⁵, N. Dzalaiova¹³, T.M. Eder ¹²⁴, R.J. Ehlers ⁷³, F. Eisenhut ⁶⁴, R. Ejima ⁹¹, D. Elia ⁵⁰, B. Erazmus ¹⁰², F. Ercolessi ²⁵, B. Espagnon ¹²⁹, G. Eulisse ³², D. Evans ⁹⁹, S. Evdokimov ¹³⁹, L. Fabbietti ⁹⁴, M. Faggin ³², J. Faivre ⁷², F. Fan ⁶, W. Fan ⁷³, T. Fang⁶, A. Fantoni ⁴⁹, M. Fasel ⁸⁶, G. Feofilov ¹³⁹, A. Fernández Téllez ⁴⁴, L. Ferrandi ¹⁰⁹, M.B. Ferrer ³², A. Ferrero ¹²⁸, C. Ferrero ^{V,56}, A. Ferretti ²⁴, V.J.G. Feuillard ⁹³, V. Filova ³⁴, D. Finogeev ¹³⁹, F.M. Fionda ⁵², F. Flor ¹³⁶, A.N. Flores ¹⁰⁷, S. Foertsch ⁶⁸, I. Fokin ⁹³, S. Fokin ¹³⁹, U. Follo ^{V,56}, E. Fragiaco ⁵⁷, E. Frajna ⁴⁶, H. Friberg ⁹⁴, U. Fuchs ³², N. Funicello ²⁸, C. Furget ⁷², A. Furs ¹³⁹, T. Fusayasu ⁹⁷, J.J. Gaardhøje ⁸², M. Gagliardi ²⁴, A.M. Gago ¹⁰⁰, T. Gahlaut⁴⁷, C.D. Galvan ¹⁰⁸, S. Gami⁷⁹, D.R. Gangadharan ¹¹⁴, P. Ganoti ⁷⁷, C. Garabatos ⁹⁶, J.M. Garcia ⁴⁴, T. García Chávez ⁴⁴, E. Garcia-Solis ⁹, S. Garetti¹²⁹, C. Gargiulo ³², P. Gasik ⁹⁶, H.M. Gaur³⁸, A. Gautam ¹¹⁶, M.B. Gay Ducati ⁶⁶, M. Germain ¹⁰², R.A. Gernhaeuser ⁹⁴, C. Ghosh¹³³, M. Giacalone

O.S. Groettvik ³², F. Grosa ³², J.F. Grosse-Oetringhaus ³², R. Grosso ⁹⁶, D. Grund ³⁴, N.A. Grunwald ⁹³, R. Guernane ⁷², M. Guilbaud ¹⁰², K. Gulbrandsen ⁸², J.K. Gumprecht ¹⁰¹, T. Gündem ⁶⁴, T. Gunji ¹²², J. Guo ¹⁰, W. Guo ⁶, A. Gupta ⁹⁰, R. Gupta ⁹⁰, R. Gupta ⁴⁸, K. Gwizdziel ¹³⁴, L. Gyulai ⁴⁶, C. Hadjidakis ¹²⁹, F.U. Haider ⁹⁰, S. Haidlova ³⁴, M. Haldar ⁴, H. Hamagaki ⁷⁵, Y. Han ¹³⁸, B.G. Hanley ¹³⁵, R. Hannigan ¹⁰⁷, J. Hansen ⁷⁴, J.W. Harris ¹³⁶, A. Harton ⁹, M.V. Hartung ⁶⁴, H. Hassan ¹¹⁵, D. Hatzifotiadou ⁵¹, P. Hauer ⁴², L.B. Havener ¹³⁶, E. Hellbär ³², H. Helstrup ³⁷, M. Hemmer ⁶⁴, T. Herman ³⁴, S.G. Hernandez ¹¹⁴, G. Herrera Corral ⁸, S. Herrmann ¹²⁶, K.F. Hetland ³⁷, B. Heybeck ⁶⁴, H. Hillemanns ³², B. Hippolyte ¹²⁷, I.P.M. Hobus ⁸³, F.W. Hoffmann ⁷⁰, B. Hofman ⁵⁹, M. Horst ⁹⁴, A. Horzyk ², Y. Hou ⁶, P. Hristov ³², P. Huhn ⁶⁴, L.M. Huhta ¹¹⁵, T.J. Humanic ⁸⁷, A. Hutson ¹¹⁴, D. Hutter ³⁸, M.C. Hwang ¹⁸, R. Ilkaev ¹³⁹, M. Inaba ¹²³, M. Ippolitov ¹³⁹, A. Isakov ⁸³, T. Isidori ¹¹⁶, M.S. Islam ⁴⁷, S. Iurchenko ¹³⁹, M. Ivanov ¹³, M. Ivanov ⁹⁶, V. Ivanov ¹³⁹, K.E. Iversen ⁷⁴, M. Jablonski ², B. Jacak ^{18,73}, N. Jacazio ²⁵, P.M. Jacobs ⁷³, S. Jadlovská ¹⁰⁵, J. Jádlovský ¹⁰⁵, S. Jaelani ⁸¹, C. Jahnke ¹¹⁰, M.J. Jakubowska ¹³⁴, M.A. Janik ¹³⁴, S. Ji ¹⁶, S. Jia ¹⁰, T. Jiang ¹⁰, A.A.P. Jimenez ⁶⁵, S. Jin ^{1,10}, F. Jonas ⁷³, D.M. Jones ¹¹⁷, J.M. Jowett ^{32,96}, J. Jung ⁶⁴, M. Jung ⁶⁴, A. Junique ³², A. Jusko ⁹⁹, J. Kaewjai ¹⁰⁴, P. Kalinak ⁶⁰, A. Kalweit ³², A. Karasu Uysal ¹³⁷, N. Karatzenis ⁹⁹, O. Karavichev ¹³⁹, T. Karavicheva ¹³⁹, E. Karpechev ¹³⁹, M.J. Karwowska ¹³⁴, U. Keschull ⁷⁰, M. Keil ³², B. Ketzer ⁴², J. Keul ⁶⁴, S.S. Khade ⁴⁸, A.M. Khan ¹¹⁸, S. Khan ¹⁵, A. Khanzadeev ¹³⁹, Y. Kharlov ¹³⁹, A. Khatun ¹¹⁶, A. Khuntia ³⁴, Z. Khuranova ⁶⁴, B. Kileng ³⁷, B. Kim ¹⁰³, C. Kim ¹⁶, D.J. Kim ¹¹⁵, D. Kim ¹⁰³, E.J. Kim ⁶⁹, G. Kim ⁵⁸, H. Kim ⁵⁸, J. Kim ¹³⁸, J. Kim ⁵⁸, J. Kim ^{32,69}, M. Kim ¹⁸, S. Kim ¹⁷, T. Kim ¹³⁸, K. Kimura ⁹¹, S. Kirsch ⁶⁴, I. Kisel ³⁸, S. Kiselev ¹³⁹, A. Kisiel ¹³⁴, J.L. Klay ⁵, J. Klein ³², S. Klein ⁷³, C. Klein-Bösing ¹²⁴, M. Kleiner ⁶⁴, T. Klemenz ⁹⁴, A. Kluge ³², C. Kobdaj ¹⁰⁴, R. Kohara ¹²², T. Kollegger ⁹⁶, A. Kondratyev ¹⁴⁰, N. Kondratyeva ¹³⁹, J. König ⁶⁴, S.A. Königstorfer ⁹⁴, P.J. Konopka ³², G. Kornakov ¹³⁴, M. Korwieser ⁹⁴, S.D. Koryciak ², C. Koster ⁸³, A. Kotliarov ⁸⁵, N. Kovacic ⁸⁸, V. Kovalenko ¹³⁹, M. Kowalski ¹⁰⁶, V. Kozuharov ³⁵, G. Kozlov ³⁸, I. Králik ⁶⁰, A. Kravčáková ³⁶, L. Krcal ³², M. Krivda ^{99,60}, F. Krizek ⁸⁵, K. Krizkova Gajdosova ³⁴, C. Krug ⁶⁶, M. Krüger ⁶⁴, D.M. Krupova ³⁴, E. Kryshen ¹³⁹, V. Kučera ⁵⁸, C. Kuhn ¹²⁷, P.G. Kuijjer ⁸³, T. Kumaoka ¹²³, D. Kumar ¹³³, L. Kumar ⁸⁹, N. Kumar ⁸⁹, S. Kumar ⁵⁰, S. Kundu ³², M. Kuo ¹²³, P. Kurashvili ⁷⁸, A.B. Kurepin ¹³⁹, A. Kuryakin ¹³⁹, S. Kushpil ⁸⁵, V. Kuskov ¹³⁹, M. Kutyla ¹³⁴, A. Kuznetsov ¹⁴⁰, M.J. Kweon ⁵⁸, Y. Kwon ¹³⁸, S.L. La Pointe ³⁸, P. La Rocca ²⁶, A. Lakrathok ¹⁰⁴, M. Lamanna ³², S. Lambert ¹⁰², A.R. Landou ⁷², R. Langoy ¹¹⁹, P. Larionov ³², E. Laudi ³², L. Lautner ⁹⁴, R.A.N. Laveaga ¹⁰⁸, R. Lavicka ¹⁰¹, R. Lea ^{132,55}, H. Lee ¹⁰³, I. Legrand ⁴⁵, G. Legras ¹²⁴, A.M. Lejeune ³⁴, T.M. Lelek ², R.C. Lemmon ^{1,84}, I. León Monzón ¹⁰⁸, M.M. Lesch ⁹⁴, P. Lévai ⁴⁶, M. Li ⁶, P. Li ¹⁰, X. Li ¹⁰, B.E. Liang-gilman ¹⁸, J. Lien ¹¹⁹, R. Lietava ⁹⁹, I. Likmeta ¹¹⁴, B. Lim ²⁴, H. Lim ¹⁶, S.H. Lim ¹⁶, S. Lin ¹⁰, V. Lindenstruth ³⁸, C. Lippmann ⁹⁶, D. Liskova ¹⁰⁵, D.H. Liu ⁶, J. Liu ¹¹⁷, G.S.S. Liveraro ¹¹⁰, I.M. Lofnes ²⁰, C. Loizides ⁸⁶, S. Lokos ¹⁰⁶, J. Lömker ⁵⁹, X. Lopez ¹²⁵, E. López Torres ⁷, C. Lotteau ¹²⁶, P. Lu ^{96,118}, W. Lu ⁶, Z. Lu ¹⁰, F.V. Lugo ⁶⁷, J. Luo ³⁹, G. Luparello ⁵⁷, M.A.T. Johnson ⁴⁴, Y.G. Ma ³⁹, M. Mager ³², A. Maire ¹²⁷, E.M. Majerz ², M.V. Makariev ³⁵, M. Malaev ¹³⁹, G. Malfattore ^{51,25}, N.M. Malik ⁹⁰, N. Malik ¹⁵, S.K. Malik ⁹⁰, D. Mallick ¹²⁹, N. Mallick ¹¹⁵, G. Mandaglio ^{30,53}, S.K. Mandal ⁷⁸, A. Manea ⁶³, V. Manko ¹³⁹, A.K. Manna ⁴⁸, F. Manso ¹²⁵, G. Mantzaridis ⁹⁴, V. Manzari ⁵⁰, Y. Mao ⁶, R.W. Marcjan ², G.V. Margagliotti ²³, A. Margotti ⁵¹, A. Marín ⁹⁶, C. Markert ¹⁰⁷, P. Martinengo ³², M.I. Martínez ⁴⁴, G. Martínez García ¹⁰², M.P.P. Martins ^{32,109}, S. Masciocchi ⁹⁶, M. Masera ²⁴, A. Masoni ⁵², L. Massacrier ¹²⁹, O. Massen ⁵⁹, A. Mastroserio ^{130,50}, L. Mattei ^{24,125}, S. Mattiazzo ²⁷, A. Matyja ¹⁰⁶, F. Mazzaschi ³², M. Mazzilli ¹¹⁴, Y. Melikyan ⁴³, M. Melo ¹⁰⁹, A. Menchaca-Rocha ⁶⁷, J.E.M. Mendez ⁶⁵, E. Meninno ¹⁰¹, A.S. Menon ¹¹⁴, M.W. Menzel ^{32,93}, M. Meres ¹³, L. Micheletti ⁵⁶, D. Mihai ¹¹², D.L. Mihaylov ⁹⁴, A.U. Mikalsen ²⁰, K. Mikhaylov ^{140,139}, N. Minafra ¹¹⁶, D. Miśkowiec ⁹⁶, A. Modak ^{57,132}, B. Mohanty ⁷⁹, M. Mohisin Khan ^{VI,15}, M.A. Molander ⁴³, M.M. Mondal ⁷⁹, S. Monira ¹³⁴, C. Mordasini ¹¹⁵, D.A. Moreira De Godoy ¹²⁴, I. Morozov ¹³⁹, A. Morsch ³², T. Mrnjavac ³², V. Muccifora ⁴⁹, S. Muhuri ¹³³, A. Mulliri ²², M.G. Munhoz ¹⁰⁹, R.H. Munzer ⁶⁴, H. Murakami ¹²², L. Musa ³², J. Musinsky ⁶⁰, J.W. Myrcha ¹³⁴, N.B. Sundstrom ⁵⁹, B. Naik ¹²¹, A.I. Nambrath ¹⁸, B.K. Nandi ⁴⁷, R. Nania ⁵¹, E. Nappi ⁵⁰, A.F. Nassirpour ¹⁷, V. Nastase ¹¹², A. Nath ⁹³, N.F. Nathanson ⁸², C. Nattrass ¹²⁰, K. Naumov ¹⁸, M.N. Naydenov ³⁵, A. Neagu ¹⁹, L. Nellen ⁶⁵, R. Nepeivoda ⁷⁴, S. Nese ¹⁹, N. Nicassio ³¹, B.S. Nielsen ⁸², E.G. Nielsen ⁸², S. Nikolaev ¹³⁹, V. Nikulin ¹³⁹, F. Noferini ⁵¹, S. Noh ¹², P. Nomokonov ¹⁴⁰, J. Norman ¹¹⁷, N. Novitzky ⁸⁶, J. Nystrand ²⁰, M.R. Ockleton ¹¹⁷, M. Ogino ⁷⁵, S. Oh ¹⁷, A. Ohlson ⁷⁴,

V.A. Okorokov ¹³⁹, J. Oleniacz ¹³⁴, C. Oppedisano ⁵⁶, A. Ortiz Velasquez ⁶⁵, J. Otwinowski ¹⁰⁶, M. Oya ⁹¹, K. Oyama ⁷⁵, S. Padhan ⁴⁷, D. Pagano ^{132,55}, G. Paic ⁶⁵, S. Paisano-Guzmán ⁴⁴, A. Palasciano ⁵⁰, I. Panasenkov ⁷⁴, S. Panebianco ¹²⁸, P. Panigrahi ⁴⁷, C. Pantouvakis ²⁷, H. Park ¹²³, J. Park ¹²³, S. Park ¹⁰³, J.E. Parkkila ³², Y. Patley ⁴⁷, R.N. Patra ⁵⁰, P. Paudel ¹¹⁶, B. Paul ¹³³, H. Pei ⁶, T. Peitzmann ⁵⁹, X. Peng ¹¹, M. Pennisi ²⁴, S. Perciballi ²⁴, D. Peresunko ¹³⁹, G.M. Perez ⁷, Y. Pestov ¹³⁹, M.T. Petersen ⁸², V. Petrov ¹³⁹, M. Petrovici ⁴⁵, S. Piano ⁵⁷, M. Pikna ¹³, P. Pillot ¹⁰², O. Pinazza ^{51,32}, L. Pinsky ¹¹⁴, C. Pinto ³², S. Pisano ⁴⁹, M. Płoskoń ⁷³, M. Planinic ⁸⁸, D.K. Plociennik ², M.G. Poghosyan ⁸⁶, B. Polichtchouk ¹³⁹, S. Politano ^{32,24}, N. Poljak ⁸⁸, A. Pop ⁴⁵, S. Porteboeuf-Houssais ¹²⁵, V. Pozdniakov ^{1,140}, I.Y. Pozos ⁴⁴, K.K. Pradhan ⁴⁸, S.K. Prasad ⁴, S. Prasad ⁴⁸, R. Preghenella ⁵¹, F. Prino ⁵⁶, C.A. Pruneau ¹³⁵, I. Pshenichnov ¹³⁹, M. Puccio ³², S. Pucillo ²⁴, S. Qiu ⁸³, L. Quaglia ²⁴, A.M.K. Radhakrishnan ⁴⁸, S. Ragoni ¹⁴, A. Rai ¹³⁶, A. Rakotozafindrabe ¹²⁸, N. Ramasubramanian ¹²⁶, L. Ramello ^{131,56}, C.O. Ramírez-Álvarez ⁴⁴, M. Rasa ²⁶, S.S. Räsänen ⁴³, R. Rath ⁵¹, M.P. Rauch ²⁰, I. Ravasenga ³², K.F. Read ^{86,120}, C. Reckziegel ¹¹¹, A.R. Redelbach ³⁸, K. Redlich ^{VII,78}, C.A. Reetz ⁹⁶, H.D. Regules-Medel ⁴⁴, A. Rehman ²⁰, F. Reidt ³², H.A. Reme-Ness ³⁷, K. Reygers ⁹³, A. Riabov ¹³⁹, V. Riabov ¹³⁹, R. Ricci ²⁸, M. Richter ²⁰, A.A. Riedel ⁹⁴, W. Riegler ³², A.G. Riffero ²⁴, M. Rignanese ²⁷, C. Ripoli ²⁸, C. Ristea ⁶³, M.V. Rodriguez ³², M. Rodríguez Cahuantzi ⁴⁴, K. Røed ¹⁹, R. Rogalev ¹³⁹, E. Rogochaya ¹⁴⁰, D. Rohr ³², D. Röhrich ²⁰, S. Rojas Torres ³⁴, P.S. Rokita ¹³⁴, G. Romanenko ²⁵, F. Ronchetti ³², D. Rosales Herrera ⁴⁴, E.D. Rosas ⁶⁵, K. Roslon ¹³⁴, A. Rossi ⁵⁴, A. Roy ⁴⁸, S. Roy ⁴⁷, N. Rubini ⁵¹, J.A. Rudolph ⁸³, D. Ruggiano ¹³⁴, R. Rui ²³, P.G. Russek ², R. Russo ⁸³, A. Rustamov ⁸⁰, E. Ryabinkin ¹³⁹, Y. Ryabov ¹³⁹, A. Rybicki ¹⁰⁶, L.C.V. Ryder ¹¹⁶, J. Ryu ¹⁶, W. Rzesza ¹³⁴, B. Sabiu ⁵¹, S. Sadhu ⁴², S. Sadovsky ¹³⁹, J. Saetre ²⁰, S. Saha ⁷⁹, B. Sahoo ⁴⁸, R. Sahoo ⁴⁸, D. Sahu ⁴⁸, P.K. Sahu ⁶¹, J. Saini ¹³³, K. Sajdakova ³⁶, S. Sakai ¹²³, S. Sambyal ⁹⁰, D. Samitz ¹⁰¹, I. Sanna ^{32,94}, T.B. Saramela ¹⁰⁹, D. Sarkar ⁸², P. Sarma ⁴¹, V. Sarritzu ²², V.M. Sarti ⁹⁴, M.H.P. Sas ³², S. Sawan ⁷⁹, E. Scapparone ⁵¹, J. Schambach ⁸⁶, H.S. Scheid ^{32,64}, C. Schiaua ⁴⁵, R. Schicker ⁹³, F. Schlepfer ^{32,93}, A. Schmah ⁹⁶, C. Schmidt ⁹⁶, M.O. Schmidt ³², M. Schmidt ⁹², N.V. Schmidt ⁸⁶, A.R. Schmier ¹²⁰, J. Schoengarth ⁶⁴, R. Schotter ¹⁰¹, A. Schröter ³⁸, J. Schukraft ³², K. Schweda ⁹⁶, G. Scioli ²⁵, E. Scomparin ⁵⁶, J.E. Seger ¹⁴, Y. Sekiguchi ¹²², D. Sekihata ¹²², M. Selina ⁸³, I. Selyuzhenkov ⁹⁶, S. Senyukov ¹²⁷, J.J. Seo ⁹³, D. Serebryakov ¹³⁹, L. Serkin ^{VIII,65}, L. Šerkšnytė ⁹⁴, A. Sevcenco ⁶³, T.J. Shaba ⁶⁸, A. Shabetai ¹⁰², R. Shahoyan ³², A. Shangaraev ¹³⁹, B. Sharma ⁹⁰, D. Sharma ⁴⁷, H. Sharma ⁵⁴, M. Sharma ⁹⁰, S. Sharma ⁹⁰, U. Sharma ⁹⁰, A. Shatat ¹²⁹, O. Sheibani ¹³⁵, K. Shigaki ⁹¹, M. Shimomura ⁷⁶, S. Shirinkin ¹³⁹, Q. Shou ³⁹, Y. Sibiriak ¹³⁹, S. Siddhanta ⁵², T. Siemiarzuk ⁷⁸, T.F. Silva ¹⁰⁹, D. Silvermyr ⁷⁴, T. Simantathammakul ¹⁰⁴, R. Simeonov ³⁵, B. Singh ⁹⁰, B. Singh ⁹⁴, K. Singh ⁴⁸, R. Singh ⁷⁹, R. Singh ^{54,96}, S. Singh ¹⁵, V.K. Singh ¹³³, V. Singhal ¹³³, T. Sinha ⁹⁸, B. Sitar ¹³, M. Sitta ^{131,56}, T.B. Skaali ¹⁹, G. Skorodumovs ⁹³, N. Smirnov ¹³⁶, R.J.M. Snellings ⁵⁹, E.H. Solheim ¹⁹, C. Sonnabend ^{32,96}, J.M. Sonneveld ⁸³, F. Soramel ²⁷, A.B. Soto-hernandez ⁸⁷, R. Spijkers ⁸³, I. Sputowska ¹⁰⁶, J. Staa ⁷⁴, J. Stachel ⁹³, I. Stan ⁶³, T. Stellhorn ¹²⁴, S.F. Stiefelmaier ⁹³, D. Stocco ¹⁰², I. Storehaug ¹⁹, N.J. Strangmann ⁶⁴, P. Stratmann ¹²⁴, S. Strazzi ²⁵, A. Sturmiolo ^{30,53}, C.P. Stylianidis ⁸³, A.A.P. Suaide ¹⁰⁹, C. Suire ¹²⁹, A. Suiu ^{32,112}, M. Sukhanov ¹³⁹, M. Suljic ³², R. Sultanov ¹³⁹, V. Sumberia ⁹⁰, S. Sumowidagdo ⁸¹, L.H. Tabares ⁷, S.F. Taghavi ⁹⁴, J. Takahashi ¹¹⁰, G.J. Tambave ⁷⁹, Z. Tang ¹¹⁸, J.D. Tapia Takaki ¹¹⁶, N. Tapus ¹¹², L.A. Tarasovicova ³⁶, M.G. Tarzila ⁴⁵, A. Tauro ³², A. Tavira García ¹²⁹, G. Tejeda Muñoz ⁴⁴, L. Terlizzi ²⁴, C. Terrevoli ⁵⁰, D. Thakur ²⁴, S. Thakur ⁴, M. Thogersen ¹⁹, D. Thomas ¹⁰⁷, A. Tikhonov ¹³⁹, N. Tiltmann ^{32,124}, A.R. Timmins ¹¹⁴, M. Tkacik ¹⁰⁵, A. Toia ⁶⁴, R. Tokumoto ⁹¹, S. Tomassini ²⁵, K. Tomohiro ⁹¹, N. Topilskaya ¹³⁹, M. Toppi ⁴⁹, V.V. Torres ¹⁰², A. Trifiró ^{30,53}, T. Triloki ⁹⁵, A.S. Triolo ^{32,30,53}, S. Tripathy ³², T. Tripathy ^{125,47}, S. Trogolo ²⁴, V. Trubnikov ³, W.H. Trzaska ¹¹⁵, T.P. Trzcinski ¹³⁴, C. Tzolanta ¹⁹, R. Tu ³⁹, A. Tumkin ¹³⁹, R. Turrisi ⁵⁴, T.S. Tveter ¹⁹, K. Ullaland ²⁰, B. Ulukutlu ⁹⁴, S. Upadhyaya ¹⁰⁶, A. Uras ¹²⁶, M. Urioni ²³, G.L. Usai ²², M. Vaid ⁹⁰, M. Vala ³⁶, N. Valle ⁵⁵, L.V.R. van Doremalen ⁵⁹, M. van Leeuwen ⁸³, C.A. van Veen ⁹³, R.J.G. van Weelden ⁸³, D. Varga ⁴⁶, Z. Varga ¹³⁶, P. Vargas Torres ⁶⁵, M. Vasileiou ⁷⁷, A. Vasiliev ^{I,139}, O. Vázquez Doce ⁴⁹, O. Vazquez Rueda ¹¹⁴, V. Vechernin ¹³⁹, P. Veen ¹²⁸, E. Vercellin ²⁴, R. Verma ⁴⁷, R. Vértesi ⁴⁶, M. Verweij ⁵⁹, L. Vickovic ³³, Z. Vilakazi ¹²¹, O. Villalobos Baillie ⁹⁹, A. Villani ²³, A. Vinogradov ¹³⁹, T. Virgili ²⁸, M.M.O. Virta ¹¹⁵, A. Vodopyanov ¹⁴⁰, B. Volkel ³², M.A. Völkl ⁹⁹, S.A. Voloshin ¹³⁵, G. Volpe ³¹, B. von Haller ³², I. Vorobyev ³², N. Vozniuk ¹³⁹, J. Vrláková ³⁶, J. Wan ³⁹, C. Wang ³⁹, D. Wang ³⁹, Y. Wang ³⁹, Y. Wang ⁶, Z. Wang ³⁹, A. Wegrzynek ³², F.T. Weiglhofer ³⁸, S.C. Wenzel ³², J.P. Wessels ¹²⁴, P.K. Wiacek ², J. Wiechula ⁶⁴, J. Wikne ¹⁹,

G. Wilk⁷⁸, J. Wilkinson⁹⁶, G.A. Willems¹²⁴, B. Windelband⁹³, M. Winn¹²⁸, J.R. Wright¹⁰⁷, W. Wu³⁹, Y. Wu¹¹⁸, K. Xiong³⁹, Z. Xiong¹¹⁸, R. Xu⁶, A. Yadav⁴², A.K. Yadav¹³³, Y. Yamaguchi⁹¹, S. Yang⁵⁸, S. Yang²⁰, S. Yano⁹¹, E.R. Yeats¹⁸, J. Yi⁶, Z. Yin⁶, I.-K. Yoo¹⁶, J.H. Yoon⁵⁸, H. Yu¹², S. Yuan²⁰, A. Yuncu⁹³, V. Zaccolo²³, C. Zampolli³², F. Zanone⁹³, N. Zardoshti³², A. Zarochentsev¹³⁹, P. Závada⁶², M. Zhalov¹³⁹, B. Zhang⁹³, C. Zhang¹²⁸, L. Zhang³⁹, M. Zhang^{125,6}, M. Zhang^{27,6}, S. Zhang³⁹, X. Zhang⁶, Y. Zhang¹¹⁸, Y. Zhang¹¹⁸, Z. Zhang⁶, M. Zhao¹⁰, V. Zhrebchevskii¹³⁹, Y. Zhi¹⁰, D. Zhou⁶, Y. Zhou⁸², J. Zhu^{54,6}, S. Zhu^{96,118}, Y. Zhu⁶, S.C. Zugravel⁵⁶, N. Zurlo^{132,55}

Affiliation Notes

^I Deceased

^{II} Also at: Max-Planck-Institut für Physik, Munich, Germany

^{III} Also at: Italian National Agency for New Technologies, Energy and Sustainable Economic Development (ENEA), Bologna, Italy

^{IV} Also at: Instituto de Física da Universidade de Sao Paulo

^V Also at: Dipartimento DET del Politecnico di Torino, Turin, Italy

^{VI} Also at: Department of Applied Physics, Aligarh Muslim University, Aligarh, India

^{VII} Also at: Institute of Theoretical Physics, University of Wrocław, Poland

^{VIII} Also at: Facultad de Ciencias, Universidad Nacional Autónoma de México, Mexico City, Mexico

Collaboration Institutes

¹ A.I. Alikhanyan National Science Laboratory (Yerevan Physics Institute) Foundation, Yerevan, Armenia

² AGH University of Krakow, Cracow, Poland

³ Bogolyubov Institute for Theoretical Physics, National Academy of Sciences of Ukraine, Kiev, Ukraine

⁴ Bose Institute, Department of Physics and Centre for Astroparticle Physics and Space Science (CAPSS), Kolkata, India

⁵ California Polytechnic State University, San Luis Obispo, California, United States

⁶ Central China Normal University, Wuhan, China

⁷ Centro de Aplicaciones Tecnológicas y Desarrollo Nuclear (CEADEN), Havana, Cuba

⁸ Centro de Investigación y de Estudios Avanzados (CINVESTAV), Mexico City and Mérida, Mexico

⁹ Chicago State University, Chicago, Illinois, United States

¹⁰ China Nuclear Data Center, China Institute of Atomic Energy, Beijing, China

¹¹ China University of Geosciences, Wuhan, China

¹² Chungbuk National University, Cheongju, Republic of Korea

¹³ Comenius University Bratislava, Faculty of Mathematics, Physics and Informatics, Bratislava, Slovak Republic

¹⁴ Creighton University, Omaha, Nebraska, United States

¹⁵ Department of Physics, Aligarh Muslim University, Aligarh, India

¹⁶ Department of Physics, Pusan National University, Pusan, Republic of Korea

¹⁷ Department of Physics, Sejong University, Seoul, Republic of Korea

¹⁸ Department of Physics, University of California, Berkeley, California, United States

¹⁹ Department of Physics, University of Oslo, Oslo, Norway

²⁰ Department of Physics and Technology, University of Bergen, Bergen, Norway

²¹ Dipartimento di Fisica, Università di Pavia, Pavia, Italy

²² Dipartimento di Fisica dell'Università and Sezione INFN, Cagliari, Italy

²³ Dipartimento di Fisica dell'Università and Sezione INFN, Trieste, Italy

²⁴ Dipartimento di Fisica dell'Università and Sezione INFN, Turin, Italy

²⁵ Dipartimento di Fisica e Astronomia dell'Università and Sezione INFN, Bologna, Italy

²⁶ Dipartimento di Fisica e Astronomia dell'Università and Sezione INFN, Catania, Italy

²⁷ Dipartimento di Fisica e Astronomia dell'Università and Sezione INFN, Padova, Italy

²⁸ Dipartimento di Fisica 'E.R. Caianiello' dell'Università and Gruppo Collegato INFN, Salerno, Italy

²⁹ Dipartimento DISAT del Politecnico and Sezione INFN, Turin, Italy

³⁰ Dipartimento di Scienze MIFT, Università di Messina, Messina, Italy

³¹ Dipartimento Interateneo di Fisica 'M. Merlin' and Sezione INFN, Bari, Italy

³² European Organization for Nuclear Research (CERN), Geneva, Switzerland

- ³³ Faculty of Electrical Engineering, Mechanical Engineering and Naval Architecture, University of Split, Split, Croatia
- ³⁴ Faculty of Nuclear Sciences and Physical Engineering, Czech Technical University in Prague, Prague, Czech Republic
- ³⁵ Faculty of Physics, Sofia University, Sofia, Bulgaria
- ³⁶ Faculty of Science, P.J. Šafárik University, Košice, Slovak Republic
- ³⁷ Faculty of Technology, Environmental and Social Sciences, Bergen, Norway
- ³⁸ Frankfurt Institute for Advanced Studies, Johann Wolfgang Goethe-Universität Frankfurt, Frankfurt, Germany
- ³⁹ Fudan University, Shanghai, China
- ⁴⁰ Gangneung-Wonju National University, Gangneung, Republic of Korea
- ⁴¹ Gauhati University, Department of Physics, Guwahati, India
- ⁴² Helmholtz-Institut für Strahlen- und Kernphysik, Rheinische Friedrich-Wilhelms-Universität Bonn, Bonn, Germany
- ⁴³ Helsinki Institute of Physics (HIP), Helsinki, Finland
- ⁴⁴ High Energy Physics Group, Universidad Autónoma de Puebla, Puebla, Mexico
- ⁴⁵ Horia Hulubei National Institute of Physics and Nuclear Engineering, Bucharest, Romania
- ⁴⁶ HUN-REN Wigner Research Centre for Physics, Budapest, Hungary
- ⁴⁷ Indian Institute of Technology Bombay (IIT), Mumbai, India
- ⁴⁸ Indian Institute of Technology Indore, Indore, India
- ⁴⁹ INFN, Laboratori Nazionali di Frascati, Frascati, Italy
- ⁵⁰ INFN, Sezione di Bari, Bari, Italy
- ⁵¹ INFN, Sezione di Bologna, Bologna, Italy
- ⁵² INFN, Sezione di Cagliari, Cagliari, Italy
- ⁵³ INFN, Sezione di Catania, Catania, Italy
- ⁵⁴ INFN, Sezione di Padova, Padova, Italy
- ⁵⁵ INFN, Sezione di Pavia, Pavia, Italy
- ⁵⁶ INFN, Sezione di Torino, Turin, Italy
- ⁵⁷ INFN, Sezione di Trieste, Trieste, Italy
- ⁵⁸ Inha University, Incheon, Republic of Korea
- ⁵⁹ Institute for Gravitational and Subatomic Physics (GRASP), Utrecht University/Nikhef, Utrecht, Netherlands
- ⁶⁰ Institute of Experimental Physics, Slovak Academy of Sciences, Košice, Slovak Republic
- ⁶¹ Institute of Physics, Homi Bhabha National Institute, Bhubaneswar, India
- ⁶² Institute of Physics of the Czech Academy of Sciences, Prague, Czech Republic
- ⁶³ Institute of Space Science (ISS), Bucharest, Romania
- ⁶⁴ Institut für Kernphysik, Johann Wolfgang Goethe-Universität Frankfurt, Frankfurt, Germany
- ⁶⁵ Instituto de Ciencias Nucleares, Universidad Nacional Autónoma de México, Mexico City, Mexico
- ⁶⁶ Instituto de Física, Universidade Federal do Rio Grande do Sul (UFRGS), Porto Alegre, Brazil
- ⁶⁷ Instituto de Física, Universidad Nacional Autónoma de México, Mexico City, Mexico
- ⁶⁸ iThemba LABS, National Research Foundation, Somerset West, South Africa
- ⁶⁹ Jeonbuk National University, Jeonju, Republic of Korea
- ⁷⁰ Johann-Wolfgang-Goethe Universität Frankfurt Institut für Informatik, Fachbereich Informatik und Mathematik, Frankfurt, Germany
- ⁷¹ Korea Institute of Science and Technology Information, Daejeon, Republic of Korea
- ⁷² Laboratoire de Physique Subatomique et de Cosmologie, Université Grenoble-Alpes, CNRS-IN2P3, Grenoble, France
- ⁷³ Lawrence Berkeley National Laboratory, Berkeley, California, United States
- ⁷⁴ Lund University Department of Physics, Division of Particle Physics, Lund, Sweden
- ⁷⁵ Nagasaki Institute of Applied Science, Nagasaki, Japan
- ⁷⁶ Nara Women's University (NWU), Nara, Japan
- ⁷⁷ National and Kapodistrian University of Athens, School of Science, Department of Physics, Athens, Greece
- ⁷⁸ National Centre for Nuclear Research, Warsaw, Poland
- ⁷⁹ National Institute of Science Education and Research, Homi Bhabha National Institute, Jatni, India
- ⁸⁰ National Nuclear Research Center, Baku, Azerbaijan
- ⁸¹ National Research and Innovation Agency - BRIN, Jakarta, Indonesia
- ⁸² Niels Bohr Institute, University of Copenhagen, Copenhagen, Denmark
- ⁸³ Nikhef, National institute for subatomic physics, Amsterdam, Netherlands

- 84 Nuclear Physics Group, STFC Daresbury Laboratory, Daresbury, United Kingdom
- 85 Nuclear Physics Institute of the Czech Academy of Sciences, Husinec-Řež, Czech Republic
- 86 Oak Ridge National Laboratory, Oak Ridge, Tennessee, United States
- 87 Ohio State University, Columbus, Ohio, United States
- 88 Physics department, Faculty of science, University of Zagreb, Zagreb, Croatia
- 89 Physics Department, Panjab University, Chandigarh, India
- 90 Physics Department, University of Jammu, Jammu, India
- 91 Physics Program and International Institute for Sustainability with Knotted Chiral Meta Matter (WPI-SKCM²), Hiroshima University, Hiroshima, Japan
- 92 Physikalisches Institut, Eberhard-Karls-Universität Tübingen, Tübingen, Germany
- 93 Physikalisches Institut, Ruprecht-Karls-Universität Heidelberg, Heidelberg, Germany
- 94 Physik Department, Technische Universität München, Munich, Germany
- 95 Politecnico di Bari and Sezione INFN, Bari, Italy
- 96 Research Division and ExtreMe Matter Institute EMMI, GSI Helmholtzzentrum für Schwerionenforschung GmbH, Darmstadt, Germany
- 97 Saga University, Saga, Japan
- 98 Saha Institute of Nuclear Physics, Homi Bhabha National Institute, Kolkata, India
- 99 School of Physics and Astronomy, University of Birmingham, Birmingham, United Kingdom
- 100 Sección Física, Departamento de Ciencias, Pontificia Universidad Católica del Perú, Lima, Peru
- 101 Stefan Meyer Institut für Subatomare Physik (SMI), Vienna, Austria
- 102 SUBATECH, IMT Atlantique, Nantes Université, CNRS-IN2P3, Nantes, France
- 103 Sungkyunkwan University, Suwon City, Republic of Korea
- 104 Suranaree University of Technology, Nakhon Ratchasima, Thailand
- 105 Technical University of Košice, Košice, Slovak Republic
- 106 The Henryk Niewodniczanski Institute of Nuclear Physics, Polish Academy of Sciences, Cracow, Poland
- 107 The University of Texas at Austin, Austin, Texas, United States
- 108 Universidad Autónoma de Sinaloa, Culiacán, Mexico
- 109 Universidade de São Paulo (USP), São Paulo, Brazil
- 110 Universidade Estadual de Campinas (UNICAMP), Campinas, Brazil
- 111 Universidade Federal do ABC, Santo Andre, Brazil
- 112 Universitatea Nationala de Stiinta si Tehnologie Politehnica Bucuresti, Bucharest, Romania
- 113 University of Derby, Derby, United Kingdom
- 114 University of Houston, Houston, Texas, United States
- 115 University of Jyväskylä, Jyväskylä, Finland
- 116 University of Kansas, Lawrence, Kansas, United States
- 117 University of Liverpool, Liverpool, United Kingdom
- 118 University of Science and Technology of China, Hefei, China
- 119 University of South-Eastern Norway, Kongsberg, Norway
- 120 University of Tennessee, Knoxville, Tennessee, United States
- 121 University of the Witwatersrand, Johannesburg, South Africa
- 122 University of Tokyo, Tokyo, Japan
- 123 University of Tsukuba, Tsukuba, Japan
- 124 Universität Münster, Institut für Kernphysik, Münster, Germany
- 125 Université Clermont Auvergne, CNRS/IN2P3, LPC, Clermont-Ferrand, France
- 126 Université de Lyon, CNRS/IN2P3, Institut de Physique des 2 Infinis de Lyon, Lyon, France
- 127 Université de Strasbourg, CNRS, IPHC UMR 7178, F-67000 Strasbourg, France, Strasbourg, France
- 128 Université Paris-Saclay, Centre d'Etudes de Saclay (CEA), IRFU, Département de Physique Nucléaire (DPhN), Saclay, France
- 129 Université Paris-Saclay, CNRS/IN2P3, IJCLab, Orsay, France
- 130 Università degli Studi di Foggia, Foggia, Italy
- 131 Università del Piemonte Orientale, Vercelli, Italy
- 132 Università di Brescia, Brescia, Italy
- 133 Variable Energy Cyclotron Centre, Homi Bhabha National Institute, Kolkata, India
- 134 Warsaw University of Technology, Warsaw, Poland
- 135 Wayne State University, Detroit, Michigan, United States
- 136 Yale University, New Haven, Connecticut, United States

¹³⁷ Yildiz Technical University, Istanbul, Turkey

¹³⁸ Yonsei University, Seoul, Republic of Korea

¹³⁹ Affiliated with an institute formerly covered by a cooperation agreement with CERN

¹⁴⁰ Affiliated with an international laboratory covered by a cooperation agreement with CERN.